CENTER FOR DRUG EVALUATION AND RESEARCH

APPLICATION NUMBER:

22-068

PHARMACOLOGY REVIEW

Memorandum

October 24, 2007

From: David Jacobson-Kram, Ph.D., DABT Office of New Drugs
To: Robert Justice, MD
Thru: John Leighton, Ph.D.

Subject: Review of pharmacology/toxicology section of NDA 22-068

I have reviewed the pharmacology/toxicology section of NDA 22-068 and the nonclinical toxicology/pharmacology section of the proposed drug label. I agree with the primary reviewer's conclusions and with the wording of the non clinical section of the package insert.

This is a representation of an electronic record that was signed electronically and this page is the manifestation of the electronic signature.

/s/

David Jacobson-Kram
10/24/2007 12:39:38 PM
PHARMACOLOGIST

MEMORANDUM

Date: October 23, 2007
From: John K. Leighton, PhD, DABT
Supervisory Pharmacologist
Division of Drug Oncology Products
To: File for NDA #22-068
TASIGNA (nilotinib)
Re: Approvability for Pharmacology and Toxicology

Nonclinical pharmacology and toxicology studies for nilotinib were provided in support of the NDA for Tasigna and were reviewed in detail by Dr. Shwu-Luan Lee. The studies consist of original research conducted by the applicant. Tasigna is indicated for the treatment chronic phase and accelerated phase Philadelphia chromosome positive CML in adult patients resistant or intolerant to prior therapy, including imatinib. The supporting studies included information of nilotinib's pharmacology; pharmacokinetic and ADME; safety pharmacology; general toxicology (rat, dog and monkey); genetic toxicity (complete ICH battery) of nilotinib and potential impurities; a fertility study in rats; embryo-fetal developmental toxicity in rats and rabbits; and phototoxicity.

Nilotinib is an inhibitor of Bcr-Abl and several other kinases. The pharmacology studies submitted to the NDA suggest that nilotinib may target wild-type and many, but not all, of the mutant forms of the Bcr-Abl kinase. Activity against some of the mutant forms of this kinase has been assessed clinically. In safety pharmacology studies, nilotinib showed some potential of cardiotoxicity, particularly activity in the hERG assay, suggesting potential inhibition of this ion channel. Other *in vitro* assays also showed some liability, but no acute cardiovascular toxicity was noted in the *in vivo* studies. In general toxicology studies, nilotinib showed greatest effect to the hepatobiliary system, a toxicity observed in clinical trials.

Nilotinib was negative for evidence of genetic toxicity in the standard battery of tests describe by ICH. In screening bacterial assays, several possible impurities were positive for mutagenesis. However, the CMC reviewer did not note any drug product impurities of concern [redacted] Carcinogenicity studies were not conducted for nilotinib, nor are they needed for use in this patient population. Nilotinib was negative for significant effects on fertility and teratogenesis. However, in the rat fertility study and the rat and rabbit embryo-fetal developmental toxicity studies, numerous drug-related effects were observed in the absence and presence of maternal toxicity. Pregnancy Category D is recommended based on embyro-fetal toxicity. The nonclinical findings are detailed in Dr. Lee's review and Executive Summary and reflected in the product label.

Recommendation: I concur with Dr. Lee's conclusion that pharmacology and toxicology data support the approval of NDA 22-068 for Tasigna. There are no outstanding nonclinical issues related to the approval of Tasigna.

This is a representation of an electronic record that was signed electronically and this page is the manifestation of the electronic signature.

/s/

John Leighton
10/23/2007 11:21:45 AM
PHARMACOLOGIST

DEPARTMENT OF HEALTH AND HUMAN SERVICES
PUBLIC HEALTH SERVICE
FOOD AND DRUG ADMINISTRATION
CENTER FOR DRUG EVALUATION AND RESEARCH

PHARMACOLOGY/TOXICOLOGY REVIEW AND EVALUATION

NDA NUMBER:	**22-068**
SERIAL NUMBER:	**000**
DATE RECEIVED BY CENTER:	**9/28/2006**
PRODUCT:	**Tasigna® (nilotinib) capsules**
INTENDED CLINICAL POPULATION:	**Imatinib-intolrant chronic myelogenous leukemia (CML)**
SPONSOR:	**Novartis Pharmaceuticals Corporation** **One Health plaza, East Hanover, NJ 07936**
DOCUMENTS REVIEWED:	**Electronic submission**
REVIEW DIVISION:	**Division of Drug Oncology Products (HFD-150)**
PHARM/TOX REVIEWER:	**Shwu-Luan Lee, Ph.D.**
PHARM/TOX SUPERVISOR:	**John Leighton, Ph.D.**
DIVISION DIRECTOR:	**Robert Justice, M.D., M.S.**
PROJECT MANAGER:	**Janet Jamison**

Date of review submission to Division File System (DFS): **August 13, 2007**

TABLE OF CONTENTS

EXECUTIVE SUMMARY

I. Recommendations

A. Recommendation on approvability
Approvable. The non-clinical studies of oral nilotinib (Tasigna®) support the safety of its use in Ph+ chronic myelogenous leukemia (CML).

B. Recommendation for nonclinical studies
No additional non-clinical studies are necessary for nilotinib for the proposed indication.

C. Recommendations on labeling
A separate review will be conducted.

II. Summary of nonclinical findings

A. Brief overview of nonclinical findings

Nilotinib (AMN107) is a kinase inhibitor that targets Bcr-Abl, c-Kit and platelet derived growth factor (PDGF) receptor, via an ATP-competitive mechanism.

Orally administered nilotinib was absorbed rapidly (T_{max} 0.5-4 hr), with bioavailability ranging from 20 to 43% in the tested rodent (mice and rats) and non-rodent (rabbits and monkeys) species. The plasma protein binding of nilotinib was high (over 97% in all tested species), and bile, uveal tract (pigment layer in the eye), stomach glandular, liver, and adrenal gland, had highest nilotinib concentration. Although nilotinib showed little penetration through the blood-brain and blood-testis barrier, it crossed the placenta and entered the fetuses. Nilotinib was found in the milk of lactating rats after a single oral dose. The biotransformation of nilotinib was primarily oxidation, oxidative cleavage of the imidazole ring, amide bond hydrolysis, and glucuronic acid conjugation. The commonly found metabolites in rat, dog, monkey and human were P20, P36, P36.5, P41.6, P42.1, P47 and P50. The rat and monkey profiles were most similar to that of human, and that in dog was the least. One of the major metabolites in human, P36.5 (approximately 7% AUC of parent drug), was also found in plasma of monkey but not other species. Cytochrome P450 (CYP) 3A4 was responsible for the hepatic oxidative clearance of nilotinib. In *in vitro* studies, nilotinib inhibited CYP 2D6, 2C19, 2C9, 3A4, 2C8, UGT1A1 and P-glycoprotein, but induced CYP 2B6, 2C8, 2C9, 3A4, 1A1, 1A2 and UGT1A1. The main excretion after oral doses was fecal. After repeated administration (4 to 39 weeks), while the accumulation was not seen in every dose group in rats, nilotinib accumulated in dogs (in both sexes at higher doses) and monkeys (in both sexes at all doses tested). The systemic exposure to nilotinib increased with dose, and was generally proportional in rats, but less than proportional in dogs and monkeys.

The safety pharmacology studies in rat, rabbit and dog, and general toxicology studies in rat, dog and monkey identified liver, bile duct, gall bladder, lung, spleen, heart and pancreas as the target organs. The major findings are as the follows:

- Hematopoietic and lymphoid systems:
  There were no remarkable histopathological change in the bone marrow, but nilotinib treatment suppressed erythroid parameters (RBC, HGB, Hct) in rats (360 mg/m^2) and monkeys (≥ 2400 mg/m^2), while increased white blood cells counts (total and differentiated) in rats (360 mg/m^2) were observed. In monkeys, nilotinib (7200 mg/m^2) increased platelet counts and prolonged APTT. The elevated white counts may be associated with infection or secondary to the drug reaction in the lymphoid tissues, as evidenced by inflammation in multiple organs, and lymphoid hyperplasia in lymph nodes and spleen. Other histopathological findings in lymphoid tissues also included: erythrocyte accumulation or erythrophagocytosis in lymph nodes, and fibrosiderotic nodule, hemorrhage, fibrosis and hypocellularity in spleen.
- Hepatobiliary system:
  Lesions in liver and bile duct were minimal in rats but observed in dogs (≥ 300 mg/m^2) and monkeys (≥ 300 mg/m^2). Lesions in gall bladder were also found in dogs (≥ 300 mg/m^2). The hepatobiliary and gall bladder toxicities were supported by observations such as: clinical chemistry (elevated ALT and/or ALP, total bilirubin and cholesterol in dogs and monkeys and ↑ triacylglyceride in monkeys), ↑ liver weight (rats and dogs), gross and histopathology (liver: enlarged, Kupffer cell hypertrophy and hyperplasia in dogs, discoloration, cytoplasmic aggregation, pigment and valuolation in sinusoidal cells, fibrosis, mononuclear cell infiltration in monkeys; bile duct: inspissation, proliferation in dogs, enlarged and hyperplasia in monkeys; gall bladder: increased luminal mucus, brown focus, lymphoid hyperplasia in dogs).
- Renal system:
  There were no specific clinical chemical or urinalysis observations associated with renal toxicities. A unique renal toxicity, hyaline droplet formation in the proximal tubules, was associated with male rats only (≥ 36 mg/m^2). Tubular cast, basophilia and vacuolation, mineralization, fibrosis were found in dogs (≥ 100 mg/m^2) and monkeys (≥ 360 mg/m^2). The renal toxicities were mild and with low incidence.
- Cardiovascular system:
  Nilotinib inhibited hERG tail current with IC_{50} at 0.13 μM. It also prolonged action potential duration (APD) and induced triangulation and beat-to-beat variability in rabbit hearts. The coronary vasoconstrictive effect was illustrated in rabbit hearts as well as in isolated human coronary arteries. However, nilotinib did not have remarkable cardio-hemodynamic effects in conscious telemetered dogs, or electrocardiography in dogs and monkeys in the toxicology studies. Increased heart weights, both absolute and relative to body weight, were observed in rats, dogs and monkeys. Nilotinib exhibited minimal histopathological changes in animals: cardiomyopathy in rats (≥ 120 mg/m^2), focal mesothelial cell proliferation and coronary medial hypertrophy in dogs (≥ 300 mg/m^2), and slight hemorrhage in monkeys (7200 mg/m^2).
- Respiratory system:
  Nilotinib did not affect respiratory functions (respiratory rate, minute volume and tidal volume values) in rats at a single oral dose up to 1800 mg/m^2. The histopathological findings in the animals included: focal hemosiderosis, macrophage accumulation, perivascular cuffing in dogs (900 mg/m^2), and interstitial inflammation, edema, leukocytic infiltration in monkeys (7200 mg/m^2).
- Other toxicities:

Nilotinib showed no effects on functions in CNS system, or histopathological lesions in the brain or other nervous system. Nilotinib caused lesions in eyes in rats (at 360 mg/m^2, anterior chamber exudates, keratitis, retrobulber hemorrhage and inflammation), at low incidence but with moderate severity. Mononuclear cell infiltration was found in eye balls/choroid in male monkeys (≥ 360 mg/m^2). Other target organs/tissues included: thyroid (fibrosis, hyperplasia, mononuclear cell infiltration) in monkeys (7200 mg/m^2), and pancreas (acinar atrophy and degeneration, inflammation) in dogs (900 mg/m^2) and monkeys (7200 mg/m^2), and GI tract (clinical findings such as salvation, fecal changes and emesis) found in all species tested. Nilotinib is also potentially phototoxic based on *in vitro* study in which nilotinib reduced the viability of UV irradiated 3T3 cells..

Nilotinib was not mutagenic or clastogenic in bacterial Ames and chromosome aberration test in human peripheral lymphocytes, and did not increase micronucleus formation in rats after oral dose up to 2000 mg/kg (12000 mg/m^2). Nilotinib was negative for DNA damage in the Comet assay. However, impurity [redacted] were positive in the bacterial mutagenicity test; although the contents of theses impurities did not exceed the regulatory threshold in the clinical batches.

Reproductive and developmental toxicities of nilotinib were investigated in rats and rabbits. Nilotinib did not affect male or female fertility, or pregnancy indices. In rats, embryofetal toxicities (at doses ≥ 180 mg/m^2) were seen in the absence of maternal toxicity (at 600 mg/m^2), while nilotinib induced dose-dependent embryo- and fetal toxicities in rabbits were associated with maternal toxicity (at 3600 mg/m^2). In rats, nilotinib increased resorption, post-implantation loss, as well as decreased viable fetuses and litter size, with decreased fetal viability at ≥120 mg/m^2. The embryo-fetal toxicities of nilotinib in rats included visceral variations, and skeletal malformations and variations. In rabbits, although inducing abortion and embryonic toxicities, nilotinib-induced fetal toxicity was mild; and only skeletal variations were noted. The finding dose of embryo-fetal toxicity in rabbits was 3600 mg/m^2. Nilotinib was not considered teratogenic.

B. Pharmacologic activity

The inhibitory effects of nilotinib to the target tyrosine kinases (Bcr-Abl fusion protein, c-Kit and PDGFRα and PDGFβ), as well as selected Bcr-Abl mutants, were characterized in *in vitro* and/or *in vivo* systems. Nilotinib inhibited the cellular activities in 32 out of 33 mutants tested. The Bcr-Abl mutants including E255K, G250E andY253H, are commonly identified in CML patients who were relapsed from or resistant to imatinib treatment. Nilotinib, however, exhibited no effects against mutant T315I, a mutant resistant to both imatinib and dasatinib.

Nilotinib (10 μM) inhibited the JAKs (Janus kinases) dependent cell proliferation (20-60%), indicating the link between Bcr-Abl and JAK pathways. JAK kinases are critical for cytokine/growth factor signaling, and may be associated with human cancer.

C. Nonclinical safety issues relevant to clinical use

The toxicities in the target organs identified in the animals, i.e., hematopoietic (anemia) and lymphoid (infections), hepatobiliary (increased liver enzymes), renal, and cardiovascular (cardiac failure, angina pectoris) systems, and other organs such as GI tract (diarrhea, abdominal pain), lung (pleural effusion), eye (hemorrhage), thyroid (hyper- or hypothyroidism) and pancreas

(increased lipase and amylase), were also reported in the patients as indicated in the parentheses. Despite the observations that nilotinib increased white blood cell or platelet counts in some species, inflammation and hemorrhage were seen in multiple organs in all species of animals tested. In light of the potential intervention of the Bcr-Abl and JAK, nilotinib can potentially compromise the host cytokine signaling and hence immune system.

Nilotinib exhibited pro-arrhythmic potential in the *in vitro* studies, despite no QT prolongation or other electrographical findings. Increased heart weights (over 10% from the control) observed in rats, dogs and monkeys may indicate potential cardiomyopathy in humans, despite minimal histopathological findings in animals. Rats treated with imatinib (Gleevec) for 6 months were found with no obvious histopathological lesions in the heart, except for increased heart weights. However, prolonged treatment of imatinib for 2 years led to cardiomyopathy in rats, a finding also reported in the patients (Kerkela *et al.*, Nature Medicine 2006, 12:908-916). Nilotinib demonstrated dose-dependent embryofetal toxicities in rats and rabbits.

Hyperbilirubinemia observed in patients may be related to the finding that AMN107 induced inhibition of UGT1A1 mediated glucuronidatiopn of bilirubin in pooled human liver microsomes.

2.6 PHARMACOLOGY/TOXICOLOGY REVIEW

2.6.1 INTRODUCTION AND DRUG HISTORY

NDA number:	22-068
Review number:	1
Sequence number/date/type of submission:	000/September 28, 2006/NDA
Information to sponsor:	Yes ( ) No (x)
Sponsor and/or agent:	Norvatis Pharmaceuticals Corporation One Health Plaza East Hanover, NJ 07936-1080
Manufacturer for drug substance:	Novartis Pharma Stein AG Schaffhauserstrasse CH-4332 Stein Switzerland

Reviewer name:	Shwu-Luan Lee, Ph.D.
Division name:	Division of Drug Oncology Products
HFD #:	HFD-150
Review completion date:	8/13/2007

Drug:

Trade name:	TASIGNA®
Generic name:	Nilotinib
Code name:	AMN 107-AAA.001, NVP-AMN107-NX (free base), NVP-AMN107-AA (monohydrate salt)
Chemical name:	4-Methyl-N-[3-(4-methyl-1H-imidazol-l-yl)-5-(trifluoromethyl)phenyl]-3-[[4-(3-pyridinyl)-2-pyrimidinyl]amino]-benzamide, monohydrochloride, monohydrate
CAS registry number:	641571-10-0 (free base)
Molecular formula:	$C_{28}H_{22}N_7OF_3 \cdot HCl, H_2O$
Molecular weight:	583.99 gm/mole (salt form monohydrate), 565.98 gm/mole (salt form anhydrous)
Structure:	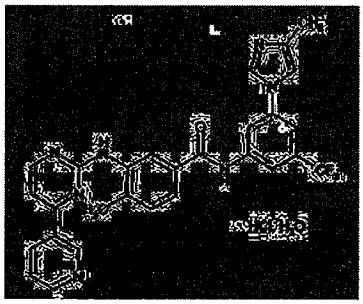

Relevant INDs/NDAs/DMFs: IND: 69764

Drug class: Receptor tyrosine kinase inhibitor of Bcr-Abl

Intended clinical population: Tasigna is "indicated for the treatment of chronic phase and accelerated phase Ph+ chronic myelogenous leukemia (CML) in adult patients resistant to or intolerant to prior therapy including imatinib."

Clinical formulation: Composition of nilotinib 200 mg capsules:

AMN107	[redacted]
Lactose monohydrate	
Cospovidone	[redacted]
Poloxamer 188	
[redacted]	[redacted]
Magnesium sterate	

Route of administration: Oral

Disclaimer: Tabular and graphical information are constructed by the reviewer unless cited otherwise.

Studies reviewed within this submission:

Primary pharmacodynamics:

RD-2004-00907: Cellular activities and selectivity profile of the Bcr-Abl kinase inhibitor NVP-AMN107-NX	pharmtox\pharm\rd-2004-00907.pdf
RD-2005-00702: Cellular activities against kinase domain mutants of Bcr-Abl	pharmtox\pharm\rd-2005-00702.pdf
RD-2006-00117: In vitro effects of NVP-AMN107 on a selection of human protein kinases and Imatinib-resistant mutants of Bcr-Abl	pharmtox\pharm\rd-2006-00117.pdf
RD-2005-01550: Efficacy of AMN107 in the 32D/Bcr-Abl/luc model	pharmtox\pharm\rd-2005-01550.pdf

Secondary pharmacodynamics:

RD-2004-00907: Cellular activities and selectivity profile of the Bcr-Abl kinase inhibitor NVP-AMN107-NX	pharmtox\pharm\rd-2004-00907.pdf
RD-2006-00117: In vitro effects of NVP-AMN107 on a selection of human protein kinases and Imatinib-resistant mutants of Bcr-Abl	pharmtox\pharm\rd-2006-00117.pdf
RD-2006-00095: Assessment of JAK inhibition by AMN107	pharmtox\pharm\rd-2006-00095.pdf

Safety pharmacology:

Nervous system:

Study 0510047: Oral safety pharmacology study in rats (nervous and respiration system)	pharmtox\pharm\0510047.pdf

Cardiovascular:

Study 0380166: Effects of AMN107 on cloned hERG channels expressed in mammalian cells	pharmtox\pharm\0380166.pdf
Study 0616144: BJA 783: Effects on hERG tail currents in stably transfected HEK293 cells	pharmtox\pharm\0616144.pdf

Study 0350152: Electrophysiological investigations in the isolated rabbit heart	pharmtox\pharm\0350152.pdf
Study 0618514: Electrophysiological investigations in the isolated rabbit heart	pharmtox\pharm\0618514.pdf
Study 0618547: BJA783: Electrophysiological investigations in the isolated rabbit heart	pharmtox\pharm\0618547.pdf
Study 0680132: Safety study to assess test compound(s) activity in human subcutaneous resistance arteries and coronary arteries	pharmtox\pharm\0680132.pdf
Study 0380165: A pharmacological assessment of the oral (gavage) administration of AMN107 on the cardiovascular system of the conscious teleme male beagle dog	pharmtox\pharm\0380165.pdf

Pharmacokinetics:

ADME:

Absorption and excretion

DMPK R0500054: Absorption, metabolism, and excretion following a single intravenous or oral dose of [14C]AMN107 in the mouse	pharmtox\pk\dmpkr0500054.pdf
ADME(US) R0300234-1: Absorption, metabolism, and excretion in rat without bile duct cannulation and biliary excretion in the rat with bile duct cannulation following an intravenous or oral dose of a single intravenous or oral dose of [3H]AMN107	pharmtox\pk\adme(us)r0300234-1.pdf
DMPK R0500055: Absorption, metabolism, and excretion following a single intravenous or oral dose of [14C]AMN107 in the rabbit	pharmtox\pk\dmpkr0500055.pdf
DMPK R0500294: Absorption, metabolism, and excretion following a single intravenous or oral dose of [14C]AMN107 in the monkeys	pharmtox\pk\dmpkr0500294.pdf

Distribution

ADME(US) R0300252: In vitro blood distribution and binding of 3H-labeled AMN107 to plasma and/or serum proteins in the rat, dog, and human	pharmtox\pk\adme(us)r0300252.pdf
DMPK R0500654: In vitro blood distribution and binding of 3H-labelled AMN107 to plasma proteins in the mouse and monkey	pharmtox\pk\dmpkr0500654.pdf

DMPK R0400674: In vitro protein binding of [3H]AMN107 in human albumin and a1-acid glycoprotein	pharmtox\pk\dmpkr0400674.pdf
ADME(US) R0400671: Tissue distribution following an oral dose of [14C]AMN107 in the rat	pharmtox\pk\adme(us)r0400671.pdf
ADME(US) R0400671-1: Amendment No. 1: Tissue distribution following an oral dose of [14C]AMN107 in the rat	pharmtox\pk\adme(us)r0400671-1.pdf
ADME(US) R0300234-2: Tissue distribution of radioactivity following a single intravenous dose of of [3H]AMN107 in the rat	pharmtox\pk\adme(us)r0300234-2.pdf
DMPK R0600047: Tissue distribution of radioactivity following an oral dose of [14C]AMN107 in the pregnant rat	pharmtox\pk\dmpkr0600047.pdf

Metabolism

ADME(US) R0400853: In vitro metabolism of AMN107 by liver S9 fraction isolated from Aroclor-induced rats	pharmtox\pk\adme(us)r0400853.pdf
ADME(US) R0300235: In vitro metabolism of [3H]AMN107 in rat, dog, monkey, human liver slices and human hepatocytes	pharmtox\pk\adme(us)r0300235.pdf

Excretion:

DMPK R0600046: Excretion in milk after a single oral dose of [14C]AMN107 in the rat	pharmtox\pk\dmpkr0600046.pdf

Drug interaction:

ADME(US)R0300236: In vitro assessment of cytochome P450 enzyme inhibition by NVP-AMN107	pharmtox\pk\adme(us)r0300236.pdf
DMPK R0500591: In vitro assessment of UTG1A1 inhibition by NVP-AMN107	pharmtox\pk\dmpkr0500591.pdf
DMPK R0300237: AMN107 Metabolic profile in human liver microsomes, contributions of cytochrome P450s to metabolism and potential for drug-drug interactions	pharmtox\pk\dmpkr0300237.pdf

DMPK R0400672: Evaluation of AMN107 as an inducer of cytochrome P450 enzymes and drug transporters in human hepatocytes	pharmtox\pk\dmpkr0400672.pdf
ADME(US) R0400241: The potential of AMN107 to inhibit P-glycoprotein in cells determined by flow cytometry	pharmtox\pk\adme(us)r0400241.pdf

Toxicology:

Single-dose toxicology:

Study 0510033: Intravenous dose-range finding study in rats	pharmtox\tox\0510033.pdf
Study 0510081: Single-dose intravenous toxicity study in rats	pharmtox\tox\0510081.pdf

Repeat-dose toxicology: Study #0370146 and #0370147 were reviewed in IND69764

Rodents:

Study 0370146: 4-week oral (gavage) toxicity study in rats with a 4-week recovery period	pharmtox\tox\0370146.pdf
Study 0580158: A 26-week oral (gavage) toxicity study in rats with a 4-week recovery period	pharmtox\tox\0580158.pdf

Non-rodent:

Study 0370147: 4-week oral (gavage) toxicity study in dogs with a 4-week recovery period	pharmtox\tox\0370147.pdf
Study 0580157: A 39-week oral (gavage) toxicity study in cynomolgus monkeys with a 4-week recovery period	pharmtox\tox\0580157.pdf

Genotoxicity:

Study 0258040: Mutagenicity test using Salmonella typhimurium stains TA98 and TA100	pharmtox\tox\0258040.pdf
Study 0412001: Mutagenicity test using Salmonella typhimurium strains TA1535,TA97a, TA98, TA100, TA102	pharmtox\tox\0412001.pdf
Study 0412101: Chromosome aberration test with human peripheral blood	pharmtox\tox\0412101.pdf

Study 0512401: Oral bone marrow micronucleus test in rats	pharmtox\tox\0512401.pdf
Study 0259011: Comet assay in vitro with L5178Y mouse lymphoma cells (letter report)	pharmtox\tox\0259011.pdf

Genotoxicity of Impurities:

Study 0358098: [redacted] AMES test	pharmtox\tox\0358098.pdf
Study 0358099: [redacted]	pharmtox\tox\0358099.pdf
Study 0513508: [redacted] AMES test	pharmtox\tox\0513508.pdf
Study 0412011: [redacted]	pharmtox\tox\0412011.pdf

Reproductive and development toxicity:

Fertility and early embryonic development:

Study 0570152: An oral (gavage) fertility and early embryonic development study in rats	pharmtox\tox\0570152.pdf

Embryo-fetal development:

Study 0570057: An oral embryo-fetal development study in rats	pharmtox\tox\0570057.pdf
Study 0570058: An oral embryo-fetal development study in rabbits	pharmtox\tox\0570058.pdf

Other toxicity studies:

Study 0517003: UV/ vis absorption spectrum for initial phototoxicity assessment	pharmtox\tox\0517003.pdf
Study 0520056: In vitro 3T3 NRU phototoxicity assay	pharmtox\tox\0520056.pdf
Study 0517020: Assessment of photosensitizing potential with the murine local lymph node assay (LLNA tier I)	pharmtox\tox\0517020.pdf

__4__ Page(s) Withheld

__✓__ Trade Secret / Confidential

_____ Draft Labeling

_____ Deliberative Process

*Withheld Track Number: Pharm/Tox-*__4__

2.6.2 PHARMACOLOGY

2.6.2.1 Brief summary

AMN107 is a multi-protein tyrosine kinase inhibitor, targeting Bcr-Abl fusion protein, c-Kit and PDGFRα and PDGFRβ, via an ATP-competitive mechanism.

In murine and human leukemic cell lines, AMN107 demonstrated inhibitory effects against Bcr-Abl autophosphorylation and Bcr-Abl mediated cell proliferation, with IC_{50} values at 20-60 nM and 8-24 nM, respectively. Similar *in vitro* inhibitory effects were also shown towards mutant forms of Bcr-Abl commonly found in Ph+ leukemias, including E255K/V, M351T, G250E, Q252H/R, Y253H/F, F317L and E355G (IC_{50}: 30-400 nM). Among these mutant forms, G250E, E255K and Y253H are most resistant to imatinib. However, AMN107 exhibited no effects against mutant T315I, a mutant that also resistant to similar tyrosine kinase inhibitors (imatinib and dasatinib). Orally administered AMN107 (16-68 mg/kg once daily, or 10-30 mg/kg twice daily) reduced tumor burden, without obvious toxicity to the host, in the 32D/Bcr-Abl/luc nude mouse model.

The inhibitory effects of AMN107 on PDGFR and c-Kit were illustrated in *in vitro* studies. AMN107 (10 μM) inhibited JAK-dependent cell proliferation (20-60% inhibition), but did not affect JAK-mediated STAT1 nuclear translocation.

AMN107 did not have effects on functions of the nervous or respiratory system. In HEK293 cells, AMN107 blocked hERG current with an IC_{50} at 0.13 μM. In isolated rabbit hearts, AMN107 up to 0.5 μM was devoid of pro-arrhythmic potential (free of TRIaD event) and did not cause action potential duration (APD) prolongation. AMN107 at concentrations ≥ 3 μM caused prolonged APD and triangulation, and at concentrations ≥ 18 μM, instability (beat-to-beat variability in APD) was observed. AMN107 had no remarkable cardiovascular effects on telemetered conscious beagle dogs. Nevertheless, AMN107 may potentially induce coronary vasoconstricton, as indicated by reduced coronary flow in the isolated rabbit hearts. The sponsor considered the clinical relevance of these findings uncertain. However, taking together the finding of reduced coronary flow in perfused rabbit heart, and the clinical reports of myocardiac infarction, the coronary vasoconstrictive potential of AMN107 is significant and should not be overlooked.

2.6.2.2 Primary pharmacodynamics

Mechanism of action:

Nilotinib (AMN107) is an inhibitor of Bcr-Abl tyrosine kinase activity. As demonstrated by x-ray crystallographic data of AMN107 in complex with unphosphorylated (inactive) human Abl kinase, AMN107 stabilized the inactive conformation of the kinase by binding in the cleft between the N- and C-terminal lobes of the kinase domain, and occupying the ATP-binding site [redacted] The figure below depicted superposition of Abl kinase with AMN107 (between P- and-A loop) bound and Abl kinase with imatinib (upper end of A-loop) bound (figure from the sponsor):

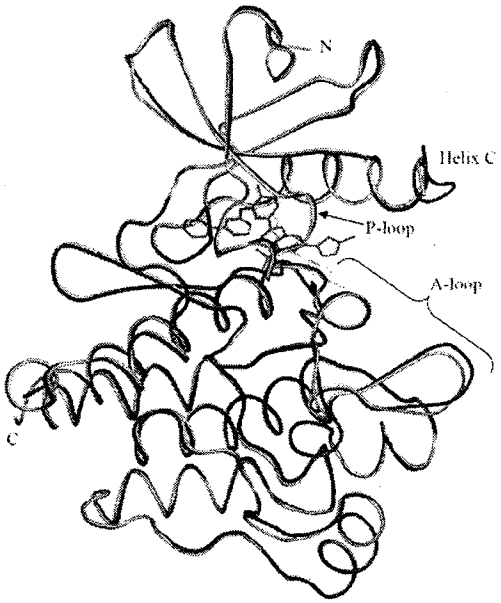

The proposed pharmacological effects of AMN107 include:

1. preventing the activation of Bcr-Abl dependent mitogenic pathway (e.g., PI_3 kinase and STAT5), leading to the death of the Bcr-Abl phenotype.
2. activity in imatinib-resistant mutants that have been identified in some relapsed patients: Glu255Val (E-255-V), Phe317Leu (F-317-L), and Met351Thr (M-351-T), but no effect on imatinib resistant T-315-I mutant.
3. inhibiting other oncogenic kinases including the FIP1L1-PDGFRα/β TK, and the stem cell factor receptor c-Kit TK.

Drug activity related to proposed indication:
In vitro studies:

- Effects of AMN107 on wild-type Bcr-Abl autophosphorylation and Bcr-Abl dependent cell proliferation *in vitro*

RD-2004-00907: Cellular activities and selectivity profile of the Bcr-Abl kinase inhibitor NVP-AMN107-NX

Key study findings: AMN107 inhibited Bcr-Abl autophosphorylation and cell proliferation at IC_{50} values in the range of 20-60 nM and 8-24 nM, respectively. AMN107 did not affect the proliferation of wild type murine cell lines in which no Bcr-Abl oncogenes was expressed.

Note: Study RD-2004-00907 contained data on both wild-type Bcr-Abl and its mutants. The study method is decribed in this section. The effects of AMN107 on Bcr-Abl mutants are reviewed in the next section. Also, the data on the effects of AMN107 against other target tyrosine kinases are reviewed under Section 2.6.2.3 "Secondary pharmadynamics".

The following cell lines were used:

- 32D cells: a murine myeloid progenitor cell line, wt-32D (32Dcl3), was transfected with the p210 Bcr-Abl expression vector pGDp210Bcr/Abl and was referred to as p210 Bcr-Abl (32D) cells in the table below.
- Ba/F3 –wt (Ba/F3): a murine IL-3 dependent pro B cell line which was transfected with p210Bcr-Abl and p185Bcr-Abl, referred to as p210 Bcr-Abl (Ba/F3) and p185Bcr-Abl (Ba/F3) cells, respectively.
- Human leukemic cell lines (Ph+ and Bcr-Abl protein expressing cell lines): K-562 and KU812F
  - K-562: a human erythroleukemia line originally isolated from a patient with CML terminal blast crisis.
  - KU812F: a subclone of human myeloblastic cell line KU812 originally established from the peripheral blood of a patient in blast crisis of CML

The phosphorylation status of the cellular targets in cell lysates, treated or untreated with AMN107 (in DMSO, 0.1%), was assessed via a capture ELISA using a c-Abl specific capture antibody.

The proliferation/viability of the Ba/F_3 cells (wild type or transfected) was determined by cell growth assays: ATPLite assay, YO-PRP-1 assay, and Alamar-Blue assay.

The table (excerpted from sponsor) shows the IC_{50} values of autophosphorylation and proliferation inhibition of AMN107 against various kinases in the cell lines tested:

Mean IC_{50} Value (nM) ± SEM (number of replicates)

Kinase (Cell Type)	Autophosphorylation	Proliferation
(wt-32D)	not applicable	6134 ± 228 (3)
(wt-Ba/F3 + IL-3)	not applicable	>10,000 (71)
p210 Bcr-Abl (32D)	20 ± 0.8 (85)	12 ± 3.0 (4)
p210 Bcr-Abl (K562)	43 ± 15 (3)	12 ± 2 (3)
p210 Bcr-Abl (KU-812F)	60 ± 19 (5)	8 ± 2 (6)
p210 Bcr-Abl (Ba/F3)	20 ± 1.6 (7)	24 ± 0.7 (75)
p185 Bcr-Abl (Ba/F3)	31 ± 3 (3)	n.a.

Manley and colleagues (Manley *et al.*, Biochim Biophy Acta 1754: 3-13, 2005) compared the effects of imatinib, dasatinib and AMN107 on autophosphorylation in a similar experiment setting as this study, and reported comparable data of AMN107 to the sponsor's result (table excerpted from the article mentioned):

Table 1
Comparison of STI571, AMN107 and BMS-354825 for effects on autophosphorylation and proliferation in cells expressing native Bcr-Abl and some of the most prevalent imatinib-resistant mutant forms of the enzymes identified in patients

Kinase (Cell Type)	STI571		AMN107		BMS-354825	
	Autophosphorylation	Proliferation	Autophosphorylation	Proliferation	Autophosphorylation	Proliferation
(*wt*-32D+IL-3)	n.a	6109±393 *n*=16	n.a	6134±228 *n*=3	n.a	Not determined
(*wt*-Ba/F3+IL-3)	n.a	>7700 *n*=4	n.a	>10,000 *n*=15	n.a	>10,000 *n*=3
Bcr-Abl (p210 32D)	192±6 *n*=94	346±43 *n*=20	19±1 *n*=68	12±3 *n*=4	1.8±0.1 *n*=4	2.6±0.1 *n*=2
Bcr-Abl (p210 Ba/F3)	221±31 *n*=14	678±39 *n*=23	20±2 *n*=7	25±1 *n*=68	1.1±0.2 *n*=3	6.4±1.5 *n*=4
G250E Bcr-Abl (p185 Ba/F3)	2287±826 *n*=4	3329±1488 *n*=2	92±10 *n*=5	145±32 *n*=3	3.7±0.5 *n*=4	7.1±3.2 *n*=2
Q252H Bcr-Abl (p185 Ba/F3)	1080±119 *n*=2	851±436 *n*=2	117±25 *n*=3	67±22 *n*=4	4.3±1.2 *n*=2	1.4±0.9 *n*=2
Y253H Bcr-Abl (p185 Ba/F3)	>10,000 *n*=2	>7000 *n*=2	260±34 *n*=6	700±116 *n*=5	2.1±0.1 *n*=4	2.7±0.1 *n*=2
E255K Bcr-Abl (p210 Ba/F3)	2455±433 *n*=4	7161±970 *n*=3	153±9 *n*=4	548±72 *n*=6	6.3±0.2 *n*=3	83±20 *n*=3
E255V Bcr-Abl (p210 Ba/F3)	6353±636 n=14	6111±854 *n*=12	244±22 *n*=13	725±55 *n*=17	4.9±1.9 *n*=3	11±1 *n*=2
T315I Bcr-Abl (p210 Ba/F3)	>10,000 *n*=22	>7000 *n*=17	>10,000 *n*=48	>10,000 *n*=51	>10,000 *n*=4	>10,000 *n*=2
F317L Bcr-Abl (p210 Ba/F3)	797±92 *n*=11	1528±227 *n*=15	38±4 *n*=13	91±6.5 *n*=17	10±3 *n*=3	38±5 *n*=2
F317V Bcr-Abl (p185 Ba/F3)	544±47 *n*=3	756±38 *n*=2	95±28 *n*=3	25±1 *n*=2	95±22 *n*=3	200±2 *n*=2
M351T Bcr-Abl (p210 Ba/F3)	593±57 *n*=11	1682±233 *n*=18	29±3 *n*=13	38±4 *n*=18	3±1 *n*=2	8±1 *n*=4
F486S Bcr-Abl (p210 Ba/F3)	1238±110 *n*=11	3050±597 *n*=10	41±4 *n*=8	75±7 *n*=11	1.5±0.6 *n*=2	10±4 *n*=3
c-Kit exon 13 mut. (GIST882)	99±10 *n*=8	106±7 *n*=14	209±14 *n*=25	160±9 *n*=21	18±2 *n*=4	55±6 *n*=4
PDGFR-α/β (A31)	72±10 *n*=12	n.a.	75±6 *n*=9	n.a.	2.9±0.4 *n*=11	n.a.
PDGFR-β (Tel Ba/F3)	n.a	44±5 *n*=11	n.a	53±5 *n*=26	n.a	2.6±0.3 *n*=4

The influence of compounds on kinase autophosphorylation or cell viability was calculated as percentage-inhibition. Dose response curves were used to calculate ED_{50} values, expressed as mean±S.E.M., *n*=number of experiments.
The influence of compounds on kinase autophosphorylation or cell viability was calculated as percentage-inhibition using the methods discussed in Section 2.1. Dose-response curves were used to calculate IC_{50} values, expressed as mean±S.E.M., *n*=number of experiments.

- Effects of AMN107 on autophosphorylation and proliferation in imatinib-resistant Bcr-Abl mutants

RD-2004-00907: Cellular activities and selectivity profile of the Bcr-Abl kinase inhibitor NVP-AMN107-NX (AMN107 free base)
RD-2005-00702: Cellular activities against kinase domain mutants of Bcr-Abl
RD-2006-00117: *In vitro* effects of NVP-AMN107 on a selection of human protein kinases and imatinib-resistant mutants of Bcr-Abl

Key study findings: AMN107 inhibited the majority of Bcr-Abl mutants tested, with IC_{50} values of autophosphorylation and Bcr-Abl mediated cell proliferation in the range of 30 to 400 nM.

Note: The effects of AMN107 on the cellular activities of Bcr-Abl were investigated in these three studies. Study RD-2004-00907 and Study RD-2006-00117 also reported data on the effects of AMN107 against other target tyrosine kinases, which is discussed under Section 2.6.2.3 "Secondary Pharmacodynamics".

Brief background of imitanib resistant Bcr-Abl mutants:
More than 35 single missense mutations in the kinase domain have been found in relapsed CML patients. The most common mutants in Ph+ leukemias are E255K/V, T315I and M351T, followed by G250E, Q252H/R, Y253H/F, F317L and E355G (Branford *et al.*, Blood 102: 276-283, 2003). This group of investigators also reported that mutants most resistant to imatinib are T315I, G250E, E255K and Y253H. Other than E255K, which may be the result of methylation-deamination reactions that give rise to C/T or G/A transitions in the context of the CpG dinucleotide sequence, these mutants appear to pre-exist and not to be induced by exposure to imatinib (Shah *et al.*, Cancer cell 2:117-125, 2002). This postulation was based on the observation of hypermutation (as a consequence of genetic instability) in the kinase domain,

multiple independent mutations (2-3 clones per patient) in 12/32 patients with imatinib resistance, and the detection of imatinib-resistant mutations in patients who were not previously exposed to, or with imatinib treatment within 1-3 months. These findings argue against an acquired mutation mechanism (Shah *et al.*, Cancer cell 2:117-125, 2002). Additionally, mutants outside of kinase domain were also identified (Azam *et al.*, Cell 112: 831-843, 2003). The mechanism of resistance is proposed to be through an allosteric destabilization of the interactions between the kinase domain and the regulatory N-terminal cap, SH3 and SH2 domains. Mutations at P-loop (the ATP binding loop) and T315I mutant are considered the most insensitive to imatinib, more aggressive, and representing a poor prognosis for patients with such mutations (Branford *et al.*, Blood 102: 276-283, 2003).

Methods:
The methods of Studies RD-2004-00907 and RD-2005-00702 were as described in the previous section. Vectors containing p210Bcr-Abl and p210Bcr-Abl kinase domain mutants such as E255K/V, E292K, T315I, F317L, M351T and F486S were transfected into Ba/F3 cells. In Study RD-2006-00117, enzyme activities were measured by the incorporation of ^{33}P ([$\gamma^{33}P$]ATP) into the peptide substrates via filter binding or flash-plate method.

Results:
The results of Study RD-2004-00907 and Study RD-2005-00702 are summarized in the table below (excerpted from sponsor):

Mean IC_{50} Value (nM) ± SEM (number of replicates)

Kinase (Cell Type)	Autophosphorylation	Proliferation
p210 E255K	170 ± 12 (6)	548 ± 72 (6)
p210 E255V	252 ± 21 (15)	791 ± 67 (19)
p210 E292K	31 ± 6 (3)	81 ± 8 (4)
p210 T315I	>8000 (57)	>10,000 (47)
p210 F317L	38 ± 4 (13)	91 ± 6.5 (17)
p210 M351T	29 ± 2.8 (13)	38 ± 3.7 (18)
p210 F486S	41 ± 3.8 (8)	75 ± 6.8 (11)
p185 (hybrid) M237I	34 (2)	35 (2)
p185 (hybrid) M244V	101 ± 16 (3)	67 ± 7 (4)
p185 (hybrid) L248V	83 ± 6.8 (3)	102 ± 13 (4)
p185 (hybrid) G250A	46 (2)	65 (2)
p185 (hybrid) G250E	92 ± 9.8 (5)	145 ± 32 (3)
p185 (hybrid) G250V	54 (2)	19 (2)
p185 (hybrid) Q252H	117 ± 25 (3)	67 ± 22 (4)
p185 (hybrid) Y253H	260 ± 34 (6)	700 ± 116 (5)

p185 (hybrid) E255D	51 (2)	24 (2)
p185 (hybrid) E255K	392 ± 82 (6)	308 ± 42 (5)
p185 (hybrid) E255R	235 (2)	56 (2)
p185 (hybrid) E275K	125 (2)	29 (2)
p185 (hybrid) D276G	107 (2)	77 (2)
p185 (hybrid) E281K	39 (2)	49 (2)
p185 (hybrid) K285N	188 (2)	63 (2)
p185 (hybrid) F311V	84 ± 1.6 (3)	155 ± 31 (4)
p185 (hybrid) F317C	57 (2)	19 (2)
p185 (hybrid) F317V	95 ± 28 (3)	28 ± 3.5 (4)
p185 (hybrid) D325N	69 (2)	25 (2)
p185 (hybrid) S348L	54 (2)	26 (2)
p185 (hybrid) E355A	91 (2)	38 (2)
p185 (hybrid) E355G	67 ± 15 (3)	47 ± 8.1 (4)
p185 (hybrid) F359C	201 (2)	291 (2)
p185 (hybrid) F359V	313 ± 79 (3)	161 ± 61 (4)
p185 (hybrid) A380S	125 (2)	179 (2)
p185 (hybrid) L387F	172 (2)	39 (2)
p185 (hybrid) M388L	68 (2)	20 (2)

These data were comparable to those reported by the Mestan *et al.* (Biochim Biophy Acta 1754: 3-13, 2005). By employing a different method to assess the effects of AMN107 on target enzyme activities, similar results were described in Study RD-2006-00117.

In vivo studies:

RD-2005-01550: Efficacy of AMN107 in the 32D/Bcr-Abl/luc model

Key study findings: Oral treatment of AMN107 in Bcr-Abl/luc model exhibited antitumor activity without affecting the host body weights.

Methods:

- CML xenograft model:
  - The Bcr-Abl expression cells were derived from 32D cells by stable transfection with vectors expressing p210Bcr-Abl fusion protein and firefly luciferase.
  - The CML model: tail vein injection of 10^5 32D/Bcr-Abl/luc cells in female mice (HsdNpa: Athymic Nude-nu, n=35).
  - To obtain the baseline luminescence, a whole body bioluminescence measurement was performed after IV injection of luciferin in tail vein 6 days after implantation of 32D cells.
- AMN107 treatment:
  - Oral (gavage) (*Reviewer's note: no information on dosing volume*)

- Dose schedule:
  - ✓ Once daily schedule: first experiment: 0, 18, 68 mg/kg (Groups 1, 2 and 3, n=8/group), second experiment: 0, 45 mg/kg (Groups 1 and 2, n=8), and third experiment: 0, 18, 45 and 68 mg/kg, for 14 days.
  - ✓ Twice daily schedule: 4th and 5th experiments: 0, 10, 20 and 30 mg/kg (Groups 1, 2, 3 and 4)
- Vehicle: 0.5% hydroxypropyl-methylcellulose (HPMC) aqueous solution containing 0.05% Tween 80. The control group received 10 mL/kg vehicle.

✧ Measurement:
- General toxicity, body weights
- Tumor burden: whole body bioluminescence measurement, on Days 4, 7 and 11 (Groups 2 and 3 only on D11) in the first experiment, and Days 7 and 13 in the second experiment.
- Antitumor activity: %T/C was calculated as (Δlight emission^{treated}/Δlight emission^{control}) x 100, where Δlight emission represented the mean emission on the evaluation day minus the mean light emission at the start of the experiment. When a negative value of Δlight emission^{treated} was obtained, this % value was marked as tumor regression (%).
- Spleen weights: mice were sacrificed at the end of experiment and spleen weights were measured to serve as an additional measurement of disease burden.
- Tissue levels of AMN107 (4th and 5th experiments only): AMN107 levels in plasma, bone marrow, spleen and liver were measured by using HPLC/MS/MS (LLOQ: 5 ng/mL for plasma and [redacted] ng/g for tissues). After 1, 6 or 12 hr following the last dose, four mice per group were sacrificed and AMN107 levels in plasma and tissues were measured (1 and 12 hr data from 4th experiment, 6 hr data from 5th experiment).

Results:

✧ Moribund sacrifice: mice in the vehicle groups were sacrificed on Day 7 in 1st and 2nd experiments, and on or after Day 11 in 3rd and 5th experiments, due to their poor condition. No moribund sacrifices were in the 4th experiment. No further information regarding toxicology findings in the moribund sacrifices was provided.

✧ Effects of AMN107 on tumor growth (light emission by luminescence measurement) and body weights: (all tables from the sponsor)

Once daily schedule:

Experiment 1: results by Day 7

Table 3-1 Evaluation of antitumor effect of NVP-AMN107 administered q.d. (1st experiment, J440)

Compound	Dose, route, schedule	Tumor response		Host response		
		T/C (%)	Regression (%)	ΔBody weight (g)	ΔBody weight (%)	Survival
Vehicle	10 ml/kg, p.o., qd	100	NA	2.8±0.5	17.5±1.4	8/8
AMN107	18 mg/kg, p.o., qd	49	NA	3.0±0.6	14.3±3.2	8/8
AMN107	68 mg/kg, p.o., qd	NA	23	3.0±0.4	14.3±2.1	7/8

Tumor burden was measured by bioluminescence. Evaluation was based on measurements from day -1 and treatment day 7 since all control animals had succumbed by day 11. Body weight evaluations are based on measurements made on day -8 and treatment day 7. Values are presented as means ± SEM.

AMN107 treatment at both doses significantly reduced tumor burden, without affecting host body weights.

Experiment 2: results on Day 7

Table 3-3 Evaluation of antitumor effect of NVP-AMN107 administered q.d. (2nd experiment J441)

Compound	Dose, route, schedule	Tumor response		Host response		
		T/C (%)	Regression (%)	ΔBody weight (g)	ΔBody weight (%)	Survival
Vehicle	10 ml/kg, p.o., qd	100	NA	-0.4±0.1	-1.9±0.3	8/8
AMN107	45 mg/kg, p.o., qd	NA	29	0.6±0.2	2.5±1.0	8/8

Tumor burden was measured by bioluminescence. Evaluation was based on measurements from treatment day 7 since all control animals had succumbed by day 11. Values are presented as means ± SEM.

A similar result as the 1st experiment was obtained at the intermediate dose.

Experiment 3: results on Day 11

Table 3-5 Evaluation of antitumor effect of NVP-AMN107 administered q.d. (3rd experiment, J519)

Compound	Dose, route, schedule	Tumor response		Host response		
		T/C (%)	Regression (%)	ΔBody weight (g)	ΔBody weight (%)	Survival
Vehicle	10 ml/kg, p.o., qd	100	NA	-1.5±1.1	6.5±4.9	3/8
AMN107	18 mg/kg, p.o., qd	91	NA	1.8±0.8	8.0±3.7	8/8
AMN107	45 mg/kg, p.o., qd	0.2	NA	1.1±0.3	4.9±1.3	8/8
AMN107	68 mg/kg, p.o., qd	NA	97	1.1±0.5	4.8±2.0	8/8

Tumor burden was measured by bioluminescence. Evaluation was based on measurements from treatment day 11 since all control animals had succumbed by day 14. Values are presented as means ± SEM.

The activity of AMN107 treatment followed dose-dependent fashion, except that the difference in tumor response (bioluminescence) between 45 mg/kg and 68 mg/kg was not statistically significant.

Twice daily schedule:

Experiment 4: results on Day 13

Table 3-7 Evaluation of antitumor effect of NVP-AMN107 administered b.i.d. (4th experiment, J542)

Compound	Dose, route, schedule	Tumor response		Host response		
		T/C (%)	Regression (%)	ΔBody weight (g)	ΔBody weight (%)	Survival
Vehicle	10 ml/kg, p.o., bid	100	NA	1.1±0.6	4.5±2.4	8/8
AMN107	10 mg/kg, p.o., bid	14	NA	1.7±0.3	7.0±1.4	8/8
AMN107	20 mg/kg, p.o., bid	0.2	NA	1.6±1.3	7.0±5.4	6/8
AMN107	30 mg/kg, p.o., bid	NA	54	1.5±0.7	5.9±2.9	8/8

Tumor burden was measured by bioluminescence. Evaluation was based on measurements from treatment day 13. Values are presented as means ± SEM.

AMN107 treatment significantly reduced tumor burden; however, there were no dose – dependent differences in this dosing regimen.

Experiment 5: results on Day 7 (figures from the sponsor)

Table 3-10 Antitumor effect of NVP-AMN107 against 32D/Bcr-Abl/luc when administered bid (5th experiment, J552)

Compound	Dose, route, schedule	Tumor response		Host response		
		T/C (%)	Regression (%)	ΔBody weight (g)	ΔBody weight (%)	Survival
Vehicle	10 ml/kg, p.o., bid	100	NA	1.9 ± 0.6	8.0 ± 2.6	8/8
AMN107	10 mg/kg, p.o., bid	35	NA	0.8 ± 0.8	3.5 ± 3.2	7/8
AMN107	20 mg/kg, p.o., bid	10	NA	1.8 ± 0.5	7.6 ± 2.0	8/8
AMN107	30 mg/kg, p.o., bid	0.03	NA	1.5 ± 0.4	6.1 ± 1.5	8/8

Tumor burden was measured by bioluminescence. Evaluation was based on measurements from treatment day 13 since all control animals had succumbed by day 11. Values are presented as means ± SEM.

Figure 3-7 Antitumor effect of twice daily administration of NVP-AMN107 against orthotopic 32D/Bcr-Abl/luc tumors (5th experiment, J552)

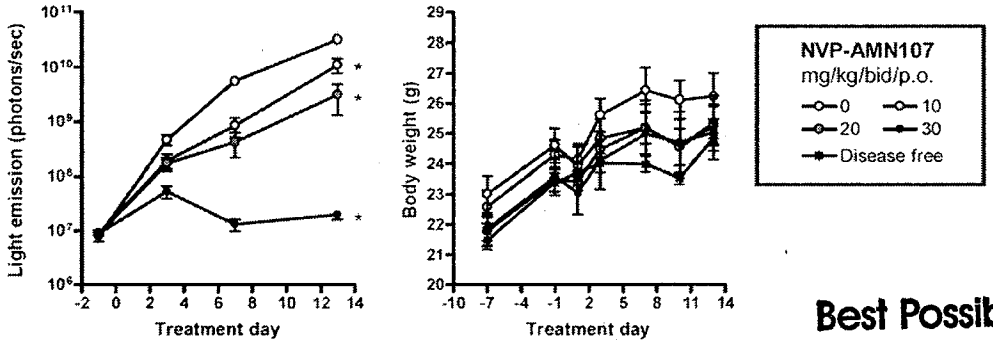

Best Possible Copy

Hematological tumors were established by intravenous injection of 105 32D/Bcr-Abl/luc cells in the tail vein of female athymic nude mice. Whole body bioluminescence was measured 6 days after inoculation and animals randomized into 4 groups (n = 8). Treatment was initiated the following day (day 0) with the indicated dosage regimen (boxed legend). Body weights and bioluminescence were recorded at regular intervals for a time period of 14 days. Animals in control group were sacrificed after on day 11 due to their poor condition. *p < 0.01 versus controls (one-way ANOVA post hoc Dunnett's)

There was no information regarding disease-free mice. There was a statistically significant difference between tumor responses comparing 10 mg/kg versus 30 mg/kg groups.

✧ The effect of AMN107 on spleen weights (following twice daily schedule) (figure and table from the sponsor)

AMN107 treatment significantly reduced spleen weights and hence spleen/body weight ratio (relative spleen weight), since AMN107 did not affect body weights. The data of disease free animals were shown as reference.

Table 3-9 Summary of spleen weight data after b.i.d treatment with NVP-AMN107

Compound	Dose, route, schedule	Spleen response				
		Spleen weight (mg)	% of vehicle	Fold over disease free	Spleen/ body weight ratio (%)	n
Vehicle	10 ml/kg, p.o., bid	829±73	100	6.2	3.3±0.34	5
AMN107	10 mg/kg, p.o., bid	165±20	20	1.2	0.63±0.063	8
AMN107	20 mg/kg, p.o., bid	120±8.3	14	0.9	0.44±0.016	6
AMN107	30 mg/kg, p.o., bid	127±9.6	15	1.0	0.47±0.027	8
Disease free	Untreated	133±8.9	16	1.0	0.54±0.038	8

Spleen weights were used as an additional measure of tumor burden at the end of the experiment (treatment day 13). Eight untreated disease free animals were includes as reference. Values are indicated as means ± SEM.

Figure 3-6 Relative spleen weight after fourteen days treatment with NVP-AMN107 in a bid schedule

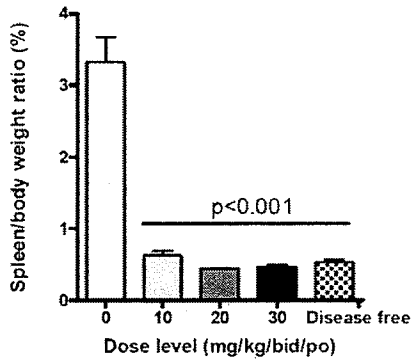

Plasma and tissue AMN107 levels (table from the sponsor)

Table 3-12 Concentration of NVP-AMN107-NX in plasma and tissues of 32D/Bcr-Abl/luc tumor bearing athymic nude mice following multiple dosing bid for 14 days (study J542, J552)

Sample matrix	Time post last dose	Dose / Schedule		
	[h]	10 mg/kg, bid	20 mg/kg, bid	30 mg/kg, bid
Plasma	A)			
[µmol/L ± SEM]	1	10.29 ± 0.83	29.42 ± 2.64	62.04 ± 6.45
[µmol/L ± SEM]	6	7.79 ± 1.41	14.78 ± 1.11	40.61 ± 5.58
[µmol/L ± SEM]	12	1.33 ± 0.29	1.92 ± 0.50	4.40 ± 1.30
Bone marrow				
[nmol/g ± SEM]	1	3.13 ± 0.50	3.80 ± 0.53	6.85 ± 0.49
[nmol/g ± SEM]	6	12.40 ± 0.51	2.62 ± 0.35	4.40 ± 0.76
[nmol/g ± SEM]	12	0.08 ± 0.06	0.06 ± 0.02	0.33 ± 0.10
Spleen				
[nmol/g ± SEM]	1	7.27 ± 0.91	9.07 ± 1.38	16.50± 3.19
[nmol/g ± SEM]	6	3.39 ± 0.23	4.97 ± 0.41	13.12 ± 1.04
[nmol/g ± SEM]	12	0.17 ± 0.02	0.22 ± 0.05	0.35 ± 0.07
Liver				
[nmol/g ± SEM]]	1	9.00 ± 0.46	25.20 ± 1.94	49.56 ± 4.13
[nmol/g ± SEM]	6	9.60 ± 1.44	12.87 ± 0.84	39.49 ± 3.07
[nmol/g ± SEM]	12	1.81 ± 0.26	2.71± 0.36	4.33 ± 0.74

Increased plasma levels correlated with higher antitumor efficacy observed in the xenograft model.

Based on the T/C (%), it appeared that similar anti-tumor activities were observed following the two dosing schedules, i.e., once daily versus twice daily..

2.6.2.3 Secondary pharmacodynamics

AMN107 was proposed to be also an inhibitor of the FIP 1-like-1 (FIP1-L1)-PDGFRα, TEL-PDGFR-β and c-Kit tyrosine kinases.

- Cellular activity and selectivity profile of AMN107 against PDGFR, c-Kit and other kinases

RD-2004-00907: Cellular activities and selectivity profile of the Bcr-Abl kinase inhibitor NVP-AMN107-NX (AMN107 free base)

RD-2006-00117: *In vitro* effects of NVP-AMN107 on a selection of human protein kinases and imatinib-resistant mutants of Bcr-Abl

Key study findings: AMN107 inhibited autophosphorylation of PDGFR and c-Kit, with IC_{50} values of 69 and 210 nM, respectively.

Note: The effects of AMN107 on cellular activities of target tyrosine kinases other than Bcr-Abl decribed in Studies RD-2004-00907 and RD-2006-00117, are reviewed in this section.

In Study RD-2004-00907 and Study RD-2006-00117, the selectivity of AMN107 on Bcr-Abl, PDGFR and C-kit TKs was demonstrated by its lack of inhibitory effects on a list of other kinases. (See Section 2.6.2.2 Drug activity related to proposed indication "In vitro studies" for experiment methods.) The table below (excerpted from sponsor) shows the selectivity profile of AMN107 according to Study RD-2004-00907.

Mean IC_{50} Value (nM) ± SEM (number of replicates)

Kinase (Cell Type)	Autophosphorylation	Proliferation
(wt-Ba/F3 + IL-3)	not applicable	>10,000 (71)
c-Kit (GIST882)	210 ± 11 (42)	158 ± 7.9 (26)
c-Kit D816V (Ba/F3)	2492 (2)	> 2900 (10)
c-Kit D816Y (Ba/F3)	480 ± 100 (3)	774 ± 135 (8)
c-Kit delVV (Ba/F3)	27 ± 2.9 (3)	26 ± 1.0 (4)
c-Kit R634W (Ba/F3)	365 ± 112 (3)	293 ± 44 (7)
PDGFR (A31)	69 ± 4.3 (47)	not determined
FIP-PDGF-Rα (Ba/F3)	not determined	2.5 – 11 (3)
Tel-PDGF-Rβ (Ba/F3)	not determined	53 ± 4.8 (26)
Alk (Ba/F3-ALK clone1)	not determined	> 3000 (3)
Akt (Ba/F3-MyrAkt clone21)	not determined	> 3000
Arg (Ba/F3 Tel-Arg)	not determined	<20 and 6
FGF-R1 (Ba/F3-Bcr-FGFR1)	not determined	> 3000 (2)
FGF-R3 (Ba/F3-TelFGFR3)	not determined	> 3000 (3)
FGF-R4 (Ba/F3-FGFR4-TD)	not determined	> 3000
Flt3-ITD (Ba/F3-NPOS-ITD)	not determined	> 3000 (3)
Flt3 N841I (Ba/F3)	not determined	> 3000
Her-1 (A431)	>3900 (6)	not determined
Her-2 (BT474)	>10000 (6)	not determined

Her-2 (Ba/F3)	not determined	>3000 (3)
Ins-R (A14)	>10000 (6)	not determined
IGF-1R (NWT-21)	>10000 (5)	not determined
IGF-1R (Ba/F3-Tel-HLH-IGF1R)	not determined	2090 ± 388 (3)
Ins-R (A14)	> 10000 (6)	not determined
Jak2 (Ba/F3-Jak2)	not determined	> 3000 (3)
Met (Ba/F3-Tpr-Met)	not determined	> 3000 (3)
Pim2 (Ba/F3-EF6-mpim2S)	not determined	> 3000 (3)
Ras (Ba/F3-H-Ras-G12V)	not determined	> 3000 (3)
Ret-Men2A (NIH3T3)	>8900 (2)	not determined
Ret (Ba/F3-PTC-3)	not determined	1754, 2463, > 3000
VEGFR-2 (CHO)	3280 ± 1038 (4)	not determined

Reviewer's note: The effects of AMN107 on autophosphorylation and cell proliferation were not assessed in all the kinases in the panel.
Point to discuss: This is the reponse to your previous question about "not determined" in the table.

The inhibition of Ephrin receptor kinase was not remarkable (Study RD-2006-00117). The IC_{50} values of nilotinib in the inhibition of enzyme activity of EphA1, EphA3, EphA4 and EphB4 were greater than 10 μM (See table below, excerpted from the sponsor's table). The sponsor considered such IC_{50} values as moderate inhibition or being inactive against the respective kinase.

Table 3-1 In vitro effects of NVP-AMN107-NX and NVP-AMN107-AA on a selection of recombinant human protein kinases

Enzyme	Type	n	Average	SD	SEM	n	Average	SD	SEM
		NVP-AMN107-AA				NVP-AMN107-NX			
EphA1	Y	4	>10	-	-	3	>10	-	-
EphA3	Y	4	>10	-	-	3	>10	-	-
EphA4	Y	4	>10	-	-	3	>10	-	-
EphB4	Y	6	>10	-	-	4	>10	-	-

Compared to the inhibitory effects of AMN107 on p210Bcr-Abl and p185Bcr-Abl (IC_{50} values for autophosphorylation and cell proliferation at the range of 20-60 nM and 8-24 nM, respectively), the inhibition of AMN107 against PDGFR approximated the former. AMN107 also exhibited inhibitory effects on c-Kit and several c-Kit mutants, except c-Kit D816V. According to data reported by Manley and colleagues (Manley *et al.*, Biochim Biophy Acta 1754: 3-13, 2005), the IC_{50} values for c-Kit autophosphorylation were 99 nM and 209 nM, and IC_{50} values for c-Kit mediated proliferation were 106 nM and 160 nM, for imatinib and AMN107, respectively. Their data also supported the investigator's study findings.

- Effects of AMN107 on Janus kinases (JAKs)

RD-2004-00907: Assessment of JAK inhibition by AMN107

Key study findings: AMN107 did not inhibit JAK dependent Ba/F3 proliferation at concentrations less than 1 μM.

Introduction:
The mammalian JAK kinases (JAK1, JAK2, JAK3 and TYK2) play a critical role in cytokine /growth factor signaling and are increasingly associated with human cancer. Imatinib has been reported to inhibit JAK2 phosphorylation by Bcr-Abl, indicating the association of these two tyrosine kinase pathways (Xie et al., Oncogene 20: 6188-6195, 2001). The effect of AMN107 on JAKs was assessed in a STAT1-GFP translocation assay in HT1080 cells and in a TEL-JAK dependent proliferation assay in Ba/F3 cells. TEL (Translocated Ets Leukemia) protein is a member of the ETS family of transcription factors whose genes are frequently rearranged in human leukemias. TEL also occurs as a tumor-associated fusion partner for tyrosine kinases ABL, PDGFR and JAK2, and results in constitutive activataion of the kinase (Majesterek *et al.*, Anti-Cancer Drugs 14: 625-631, 2003; Sjoblom *et al.*, Oncogene 18: 7055-7062, 1999).

Methods:
- ✧ Interferon-γ (IFNγ) induced, JAK2-dependent STAT1 phosphorylation and nuclear translocation was quantified by measuring the ratio of the GFP (green fluorescent protein) signaling in the cytoplasm and the nucleus in HT1080 cells transfected with a STAT1-GFP fusion construct.
- ✧ Interleukine-3 (IL3)-dependent Ba/F3 cells were transformed by integration of TEL-fusion of JAKs. The expression of TEL-activated JAKs conferred cytokine independence. In contrast, the proliferation of Ba/F3 wild-type cells was IL-3 dependent. Cytokine-independent, but JAK dependent, proliferation in the presence or absence of AMN107 was determined by the resazurin (AlamarBlue) assay.
- ✧ Ba/F3 cells expressing a JAK mutant (EpoR-JAK2V617F): Ba/F3 cells were transfected with full length JAK2V617F cDNA together with the erythropoietin receptor, which rendered the cells cytokine independent.

Results:
- ✧ STAT1 nuclear translocation assay

AMN107 up to 10 μM did not affect JAK2 mediated STAT1 translocation (figure from the sponsor):

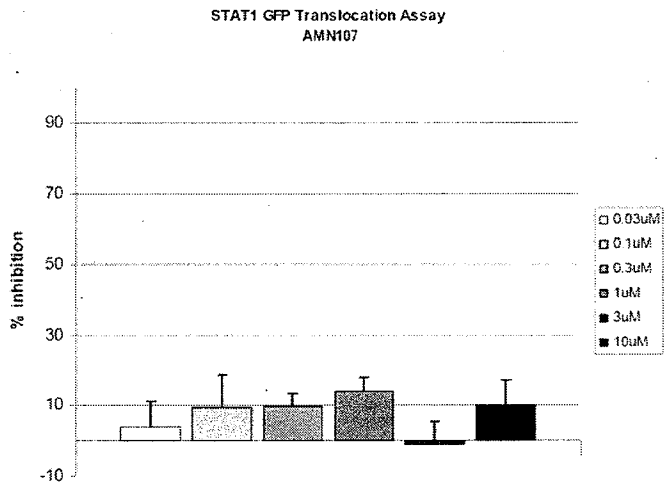

✧ Inhibition of Ba/F3 cell proliferation

The effects of AMN107 on JAK/Flt-3 transformed (positive control), TEL-JAKs transformed, and wild type Ba/F3 cells was determined (figure from the sponsor):

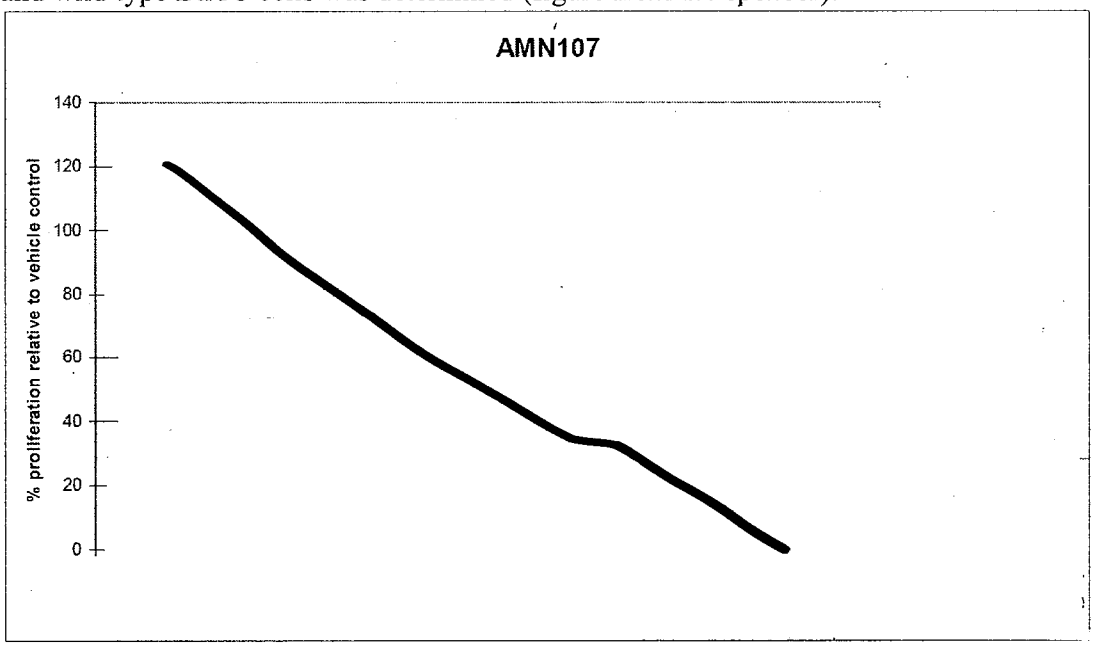

AMN107 treatment did not affect the positive control cells (Ba/F3 FLT (ITD) cells) or Ba/F3 cells expressing a JAK mutant (EpoR-JAK2V617F). AMN107 did not inhibit JAK dependent Ba/F3 proliferation at concentrations less than 1 μM. However, at 10 μM, AMN107 inhibited the proliferation of wild type or JAKs-transformed cells with inhibition ranged from 60% (JAK1 derivatives) to 20% (JAK3 derivatives).

2.6.2.4 Safety pharmacology

Neurological effects:

Study #0510047: Oral safety pharmacology study in rats (nervous and respiratory system)

Key study findings: Single oral dose of AMN107, up to 300 mg/kg, did not have effects on nervous or respiratory system.

Methods and results:
Animals: Male rats ([redacted] :W1 (Han))

Study	Treatment	Dose (mg/kg)	Dosage volume (Gavage, mL/kg)	Animal allocation	Results
Plethysmography (respiratory rate, minute volume and tidal volume values based on plethysmography data)	Vehicle (a) AMN107 (b)	0 30 300	5	n=10/group	Not remarkable
FOB observations (functional observation battery)	Vehicle AMN107	0 300	5	n=10/group	Not remarkable,

(a): 0.5% (w/v) hydroxylpropylmethylcellulose (HPMC), (b): AMN107 (batch#0523025, salt:base ratio 1.103)

Cardiovascular effects:
Study #0380166: Effects on cloned hERG channels expressed in mammalian cells

Key study findings: AMN107 inhibited hERG current with an IC_{50} of 0.13 μM.

Note: This study was reviewed in IND69764 (Review #1). The IND review is reformatted and incorporated in this NDA review.

The vehicle was HB-PS +DMSO (at a final concentration of 0.3%). Terfenadine ([redacted] 60 nM which blocks hERG current by approximately 80%) served as the positive control. Four concentrations of AMN107 were used to construct a dose-response relationship. The results are summarized in the following tables.

Concentration (μM, n=3)	0.03	0.1	0.3	1
% inhibition of I_{kr}	14.9 ± 2	43.9 ± 0.7	70.4 ± 2.5	89.7 ± 1.6

IC_{25}	IC_{50}	IC_{75}
0.04 μM	0.13 μM	0.4 μM

N: number of observation

Temperature-dependence:
The table below shows the result of raising temperature on the blockade effect of AMN107 on hERG current (data excerpted from the sponsor's report):

Table: Percentage of hERG current inhibited after application of 0.1 μM AMN107 at room temperature (18 °C-24 °C) and 35 ± 2 °C

Temperature (°C)	18-24	35 ± 2
Data #1	42.8%	43.8%
Data #2	45.3%	50.0%
Data #3	45.3%	

Mean ± SD	43.9 ± 1.3%	46.9 ± 4.4%

At 0.1 μM, the inhibitory effect of AMN107 on the hERG current did not change (from 44% to 47%) when temperature was raised from room temperature to 35 °C.

Study #0616144: BJA 783: Effects on hERG tail currents in stably transfected HEK293 cells

An AMN107 metabolite, BJA783 (P36.5) (30 μM), was incubated with HEK293 cells and produced a residual hERG tail current of 95%. In comparison, the residual current produced by the DMSO control was 99.7%, and 92.4% by the reference control, E-4031. Thus, BJA783 induced a decrease of 5% of hERG current, which is considered non-significant.

Study #0350152: Electrophysiological investigations in the isolated rabbit heart

Key study findings: The effects of AMN107 on APD prolongation in this study are inconclusive.

Note: This study was reviewed in IND69764 (Review #1). The IND review is reformatted and incorporated in this NDA review.

Isolated rabbit hearts, perfused according to the Langendorff technique in [redacted] test system, were used to investigate the effect of AMN107 on APD (AP duration) and reverse rate-dependency of APD. In addition, the conducting velocity, the AP shape (the repolarization rate, called triangulation) and the variability of APD was also determined. The concentrations of AMN107 used were 0.16, 0.48, 1.6, 4.8, 9.6 μg/mL (or, 0.3, 0.9, 3, 9 and 18 μM) in experiments 15875 and 15877, and 0.16, 0.48, 1.6, 4.8, 16 μg/mL (0.3, 0.9, 3, 9 and 30 μM) in experiment 15885. The compound precipitated at 18 μM.

Depending on individual experiment different results were obtained. The electrophysiological effects of AMN107 (in μM) were summarized in the table below:

Experiment	↓ Coronary perfusion rate	↑ APD	Triangulation	Instability
15875	≥ 0.9	≥ 9		
15877	≥ 18	≥ 3	3, 9 and 18	18
15885		≥ 9	3 and 9	30

It is difficult to draw a conclusion from this study due to the inconsistent results. However, AMN107 did not exert electrophysiological effects in the rabbit heart up to the concentration of 0.3 μM, but at ≥ 3 μM it may result in APD prolongation.

Study #0618514: Electrophysiological investigations in the isolated rabbit heart

Key study findings: AMN107 at concentration up to 0.5 μM did not show pro-arrhythmic potential, but significantly reduced coronary flow at 0.5 μM, where precipitation was observed.

The cardiac electrophysiological effects of AMN107 were investigated in 6 isolated Langendorf perfused female rabbit hearts (the SCREENIT.7 system). The hearts were incubated for 30 min with AMN107 at 0.005, 0.015, 0.05, 0.15 and 0.5 μM. Precipitation occurred at the concentrations of 0.15 and 0.5 μM

The following parameters were measured: automaticity and escape cycle length, threshold stimulation current, coronary perfusion rate, ectopic activity, left ventricular septal and epicardial monophasic action potential duration at 30, 60 and 90% of repolarization (i.e., APD_{30}, APD_{60} and APD_{90} respectively), conduction time, TRIaD events (i.e., triangulation (APD_{90}-APD_{30}), reverse use-dependence, and instability (beat-to-beat variability in APD)) that often lead to dispersion of repolarization (beat-to-beat variability between septal and epicardial APD_{60}). In addition, beat-to-beat variability of the repolarization time was measured as a Poincare plot ($PC_{30\text{-}90}$) where the sum of the distance to the diagonal was computed at each concentration. The development and number of early after depolarizations and Torsade de Pointes were detected by an automated computer algorithm. The pro-arrhythmic potential of AMN107 was estimated by the occurrence of TRIaD events and the accompanied changes of the APD.

AMN107 at 0.5 μM significantly decreased coronary flow: (figure from the sponsor)

Figure 5-1 Effects of AMN107 upon coronary flow (ml/min)

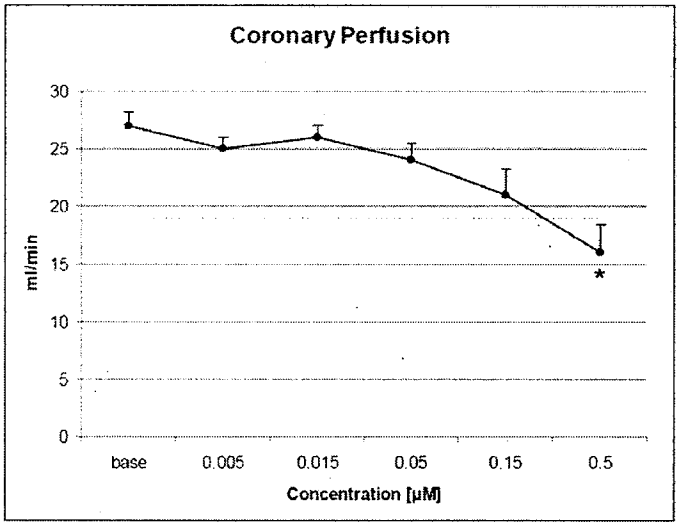

***: statistically significant by ANOVA test (p<0.05).**

The reduction of coronary flow may be due to the formation of micro-emboli at higher concentration of AMN107, when precipitation occurred.

AMN107 at concentrations up to 0.5 μM did not affect APD_{30}, APD_{60} or APD_{90}, and was devoid of TRIaD events over the test concentration range. When plotting ectopic beats against AMN107 concentrations, there were no significant changes as compared to the control.

However, there was one episode of spontaneous ventricular fibrillation accompanied by a marked reduction of coronary flow (↓ 61%) in one rabbit heart at AMN107 concentration of 0.5 μM. The investigator considered the event AMN107 related, but may be an indirect effect secondary to reduced coronary flow. A marked reduction of coronary flow (↓ 38%) also was observed in another rabbit heart, while no spontaneous ventricular fibrillation took place. Reduced coronary flow at 0.5 μM may also be attributable to a trend of slowing of conduction found at this concentration; however, it was reversible and not statistically significant.

Study #0618547: BJA783: Electrophysiological investigations in the isolated rabbit heart

Key study findings: BJA783 did not affect QT interval prolongation or other related arrhythmic risks, and did not induce any eletrophysiological effects on the tested parameters.

The AMN107 metabolite, BJA783 (P36.5), was tested for an elctrophysiological effect in 6 isolated Langendorf rabbit hearts in the [redacted] model (see above). The concentrations used were 0.02, 0.06, 0.2, 0.6 and 2 μM. The following parameters were measured: monophasic action potentials (MAP) duration at 60% repolarization (APD_{60}), reverse use-dependency, instability, triangulation, proarrhythmia index, coronary perfusion rate, intraventricular conduction, variability in pacemaker activity and amplitude of the threshold stimulation current. The statistical analysis was performed on 6 experiments using an ANOVA test.

Study CAC002/Novartis reference #0680132: Safety study to assess test compound(s) activity in human subcutaneous resistance arteries and coronary arteries

Key study findings: AMN107 at 3 μM induced vasoconstriction in the coronary artery.

The direct vascular contractile effects of AMN107 were investigated in isolated human peripheral resistance arteries (small subcutaneous arteries) and coronary arteries. All vessel segments were pre-exposed to high potassium solution (62.5 mM) to provide a reference contraction. AMN107 (dissolved in DMSO to make final solutions at 1, 3 and 10 μM in RPMI), vehicle (with DMSO at three concentration equivalents) and positive controls ANG (angiotensin) II (10 μM) or norepinephrine (1 μM) were incubated with individual vessel segment at 37°C. Responses to test article were expressed as a percentage of the high potassium solution-induced contraction (% of KPSS max).

The results are summarized in the table below (from the sponsor):

Table 4-1 Subcutaneous resistance artery raw data and patient numbers for each group

Treatment group	Changes in tone (% of KPSS Max)		
	Mean	SEM	N
1 µM AMN107	4.24	1.20	4
3 µM AMN107	-1.05	5.89	4
10 µM AMN107	9.20	9.23	4
1 µM vehicle	-18.45	13.13	4
3 µM vehicle	22.06	7.72	4
10 µM vehicle	21.31	9.08	5
10 µM Angiotensin II	210.75	75.33	4
1 µM norepinephrine (RPMI)	117.32	39.00	3
1 µM norepinephrine (PSS)	157.85	29.11	2

Table 4-2 Coronary artery raw data and patient numbers for each group

Treatment group	Changes in tone (% of KPSS Max)		
	Mean	SEM	N
1 µM AMN107	17.81	11.60	4
3 µM AMN107	55.07	9.83	4
10 µM AMN107	21.25	24.00	4
1 µM vehicle	35.92	9.38	3
3 µM vehicle	26.14	17.16	3
10 µM vehicle	23.65	25.08	4
10 µM Angiotensin II	123.49	10.77	4
1 µM norepinephrine (RPMI)	129.06	73.25	2
1 µM norepinephrine (PSS)	141.88		1

Study #0690202/ Novartis reference #0380165: A pharmacological assessment of the oral (gavage) administration of AMN107 on the cardiovascular system of the conscious telemetered male beagle dog

Key study findings:

- AMN107 at a single oral dose up to 300 mg/kg did not show electrocardiographic evidence of cardiotoxicity in telemetered conscious dogs.
- There was no treatment-related mortality, clinical signs or hemodynamic changes.

Note: This study was reviewed in IND 69764. The IND review is reformatted and incorporated in this NDA review.

Telemetry study in the conscious male Beagle dogs (n=4/group in AMN107-treated animals) showed that AMN107 at doses of 30, 100 or 300 mg/kg orally did not result in treatment – related clinical signs, nor in any changes in hemodynamic or electrocardiographic parameters. The following table shows the study design:

Table 3-1 Study design, animal allocation and test article dosages

Group no.	No. animals (males)	Test article	Dosage level (mg/kg) (Salt)[b]	Dose concentration (mg/mL) (Salt)[b]	Dosing regimen (days)	Route	Monitored period
1	1	Vehicle	0	0	1, 8, 18 and 23	Oral, via gavage[a]	24 hours post each treatment
2	4	Vehicle	0	0	1		
		AMN107	30 (32)	6 (6.4)	8		
			100 (107)	20 (21.4)	18		
			300 (321)	60 (64.1)	23		

[a] The dose volume was 5 mL/kg.
[b] Salt/base ratio was 1.069

The Group 1 animal served as a control receiving only the vehicle on each of the dose periods. All Group 2 animals initially received the vehicle (Day 1) and then received each of three escalating doses. Doses were administered with at least a 2-day washout period between the beginning of one and the start of the next.

The following in-life examinations were performed:

- Mortality and Clinical signs: twice daily
- Body weight: recorded randomLy prior to dosing. The data were filed but not reported.
- Hematology and clinical chemistry: once in pretreatment period
- Cardiovascular studies:
  - Data (systolic, diastolic, mean blood pressure, heart rate and electrocardiograms) were collected for 5 minute intervals at the following time points: on four occasions prior to each dose (24, 23, 20 and 18 hours), and on 10 occasions (30 min, 1, 2, 3, 4, 5, 6, 7, 8, and 24 hours) following each dose.
  - Electrocardiograms: PR, RR, QRS, QT, QTc and ST-elevation measurements.

Pulmonary effects: See above "neurological effects".

Renal effects: No studies conducted.

Gastrointestinal effects: No studies conducted.

Abuse liability: No studies conducted.

Other: None

2.6.2.5 Pharmacodynamic drug interactions

No studies conducted.

2.6.3 PHARMACOLOGY TABULATED SUMMARY

- Pharmacodynamics:

Summary of the inhibitory effects of AMN107 in biological assays- IC_{50} values (Means, nM) (*in vitro* system)

Assay systems	Parameters	
	Autophosphorylation	Proliferation
Murine cell lines (32D & Ba/F3) and human cell lines (K562 & KU812F)		
p210 Bcr-Abl	20-60	8-24
p185 Bcr-Abl	31	ND
Mutant forms of Bcr-Abl	30-400	20-800
Murine cell lines (Ba/F3) or others		
PDGFR (A31)	69	ND
FIP-PDGFRα	ND	2.5-11
Tel-PDGFRβ	ND	53
c-Kit (GIST882)	210	158
c-Kit mutants	27-480	26-774

ND: not determined

- Safety pharmacology

In Vitro Studies			
Study #	System	Concentrations	Results
0380166	hERG currents	AMN107: 0.03, 0.1, 0.3 and 1 μM	IC_{50}: 0.13 μM
0616144	hERG currents	BJA783 (P36.5): 30 μM	No inhibitory effects
0350152	Isolated rabbit hearts	AMN107: 0.3, 0.6, 3, 9, and 18 μM	➢ ↓ Coronary perfusion rate: ≥ 0.9 μM ➢ ↑ APD: ≥ 3 μM ➢ Triangulation: ≥ 3 μM
0618514	Isolated rabbit hearts	AMN107: 0.005, 0.015, 0.05, 0.15 and 0.5 μM	➢ No pro-arrhythmic potential ➢ ↓ coronary flow and ventricular fibrillation (1/6 hearts): 0.5 μM
0618547	Isolated rabbit hearts	BJA783 (P36.5): 0.02, 0.06, 0.2, 0.6 and 2 μM	No remarkable effects
0680132	Isolated human subcutaneous resistance and coronary arteries	AMN107: 1, 3 and 10 μM	↑ Contraction response in subcutaneous (1 μM) and coronary (3 μM) arteries
In Vivo Study			
Study #	System	Doses	Results
0510047	Nervous and respiratory: ➢ Plethysmograph (respiratory rate, minute and tidal volumes) ➢ Functional observation battery	Orally administered male rats ➢0, 30, 300 mg/kg (n=10/dose) ➢0, 300 mg/kg (n=10/dose)	No remarkable effects
0380165	Cardiovascular: telemetry in conscious male dogs	Oral doses of 0, 30, 100 and 300 mg/kg	No electrocardiographic evidence of cardiotoxicites, such as QT prolongation.

To here

2.6.4 PHARMACOKINETICS/TOXICOKINETICS

2.6.4.1 Brief summary

The pharmacokinetics of orally and intravenously administered AMN107 was investigated in the mouse, rats, rabbits, dogs and humans. ADME parameters were determined following a single dose administration, while data of toxicokinetics reported the PK profiles of AMN107 after

repeated dose administrations. Orally administered AMN107 was absorbed rapidly (T_{max} 0.5-4 hr), with bioavailability ranged from 20-43%. The IV administered radio-labeled AMN107 was broadly distributed to many tissues/organs (Vss ranged from 0.52 to 7.9 L/kg) with uveal tract, glandular stomach, liver and adrenal gland having the highest distributions. The major metabolic pathways included oxidation (methyl-imidazole ring and the pyridinyl-pyrimidine moiety), oxidative cleavage (methyl-imidazole ring), amide bond hydrolysis, and glucuronic acid conjugation of primary metabolites. Hepatic oxidative clearance of AMN107 was attributed to cytochrome P450 (CYP) 3A4. The main route of excretion of oral doses was fecal.

Based on an approximately 2 fold increase of AUC at the end of repeated administration, it appeared that, while the accumulation was not seen in every dose group in rats, AMN107 accumulated in dogs (in both sexes at higher doses) and monkeys (in both sexes at all doses tested). The systemic exposures (AUC) increased with dose, and were generally proportional in rats, but under-proportional in dogs and monkeys.

2.6.4.2 Methods of Analysis

[see under individual study reviews]

2.6.4.3 Absorption

DMPK R0500054: Absorption, metabolism, and excretion following a single intravenous or oral dose of [^{14}C]AMN107 in the mouse

Key study findings:

- Orally administered AMN107 was absorbed rapidly. AMN107 was eliminated mainly through extensive metabolism, and excreted mainly via feces.
- The major circulating components in the plasma were AMN107 (80% AUC).

Study system:	Male CD-1 mice
Treatment:	[^{14}C]AMN107 (specific activity: 13.5 µCi/mg) orally (gavage) or intravenously
Parameters:	Plasma AMN107 levels, metabolite profile, radioactivity recovery, absorption and oral bioavailability Absorption (%) = ($AUC_{0-\infty,po}$ x Dose $_{iv}$)/ ($AUC_{0-\infty,iv}$ x Dose $_{po}$)
Schedule:	Blood samples were collected predose (n=3/time point), and at 0, 0.083 (5 min), 0.25, 0.5, 1, 2, 4, 6, 8, 12, 24, 48, 72, and 96 hr post dose, and urine/feces samples collected for 0-24, 24-48, 48-72, 72-96 and 96-168 hr intervals.
Analysis:	AMN107 plasma levels (LLOQ 2.5 ng/mL) by HPLC/MS/MS, and metabolite profiling/structural characterization were determined by LC/(TOF) MS/MS analysis with off-line radioactivity. The radioactivity was determined by liquid scintillation.

- PK parameters:

	Oral (25 mg/kg)			IV (10 mg/kg)		
	Plasma AMN107	Radioactivity		Plasma AMN107	Radioactivity	
		Blood (a)	Plasma (a)		Blood (a)	Plasma (a)
$AUC_{0-\infty}$	36.1 µg•h/mL	46.7	69.7	33.8 µg•h/mL	39.8	56.5
C_{max}	21.2 µg/mL	10.5	15.1	7.9 µg/mL	21.4	29.6
T_{max} (hr)	0.5	0.5	0.5	0.083	0.083	0.083
Terminal $t_{1/2}$ (hr)*	0.9	18	9.9	1.2	20	8.8
CL (L/h/kg)	----	----	----	0.3	----	----
Vss (L/kg)	----	----	----	0.52	----	----
Absorption (%)	~49	----	----	Not applicable	----	----
Bioavailability (%)	43	----	----	Not applicable	----	----

*** Apparent terminal $t_{1/2}$ for radioactivity detection**
(a): AUC and C_{max}: µgEq•h/mL and µgEq/mL, respectively.

- Excretion and radioactivity recovery:

	Oral (25 mg/kg)	IV (10 mg/kg)
Excretion (AMN107, % dose)		
In urine (0-48 h)	Not detected	Not detected
In feces (0-48 h)	18.3	3.15
Excretion (% dose)		
Total radioactivity recovery	97.7	85.1
In urine		
0-48 h	5.72	7.67
0-168 h	5.89	7.87
In feces		
0-48 h	91.5	74.9
0-168 h	91.8	76.8
Cage wash	0.020	0.249

The primary metabolic pathways included:

- Hydroxylation: methyl group on the methyl-imidazole ring (P42.1, P31A) and the amino-benzamide moiety with further oxidation to aldehyde and carboxylic acid (P36.5)
- Oxidative cleavage: methyl-imidazole ring
- Oxidation: pyridinyl-pyrimidine moiety
- Amide bond hydrolysis (carboxylic acid metabolite: P20)

The secondary metabolic pathways included:

- Degradation of the oxidized imidazole ring
- Glucuronic acid conjugation of primary metabolites: P13A (P20 glucuronic acid conjuguate)
- Various combinations of primary and secondary pathways.

The figure below depicts these biotransformation pathways in tritium-labeled AMN107 (Figure from the sponsor):

Figure 4-2 Major metabolic reactions of [3H]AMN107

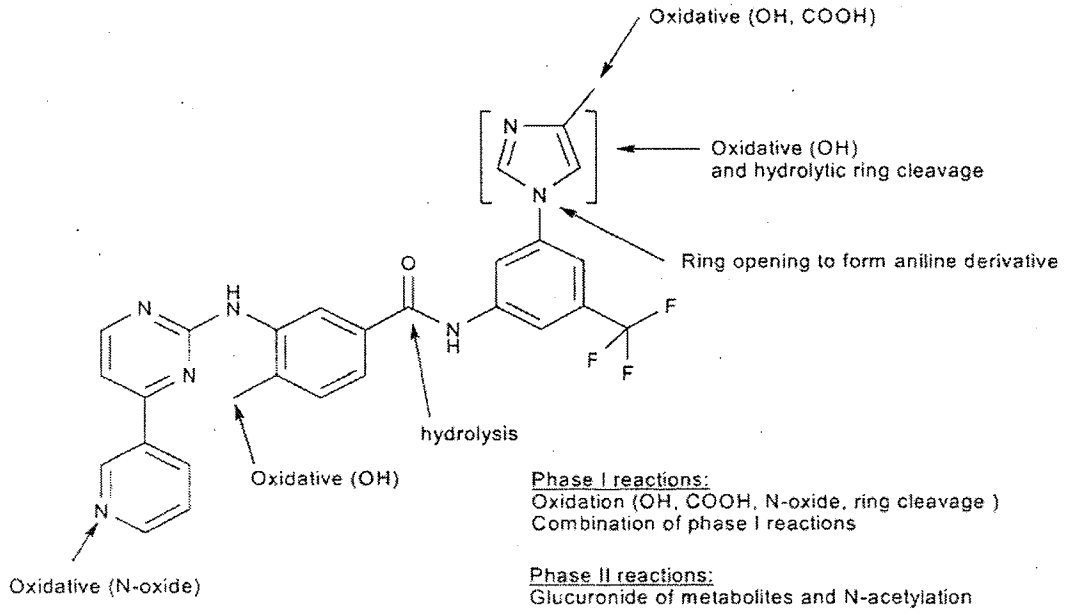

The proposed metabolic pathway of AMN107 in mouse can also be found in the figure in Section 2.6.5 (Page 67). The profile of parent drug and metabolites in the circulation is summarized in the table on Page 68 (Plasma AUC% of nilotinib and circulating metabolites after an oral radiolabeled dose in various species, from the sponsor). The major circulating component in the plasma after one single oral dose was AMN107 (80% of total AUC).

Point to discuss: best place for this summary table, because the statement of major circulating compounds (parent drug and/or the metabolites) in various species was in the key study findings.

ADME (US) R0300234-1: Absorption, metabolism, and excretion in the rat without bile duct cannulation and biliary excretion in the rat with bile duct cannulation following an intravenous or oral dose of [^{3}H]AMN107

Key study findings:

- Orally administered AMN107 was absorbed rapidly and excreted in feces.
- Elimination of AMN107 exhibited a biphasic pattern with a prolonged $t_{1/2\beta}$.
- The major circulating component in the plasma was AMN107 (84% AUC).

Study system:	Male HanWistar rats
Treatment:	[^{3}H]AMN107 (specific activity: 25.7 and 83-107 μCi/mg for oral and IV, respectively) orally (gavage) or intravenously.
Parameters:	Plasma AMN107 levels, metabolite profile, radioactivity recovery, absorption and oral bioavailability
Bile excretion:	In a separate group of rats (n=6) the bile duct was cannulated. The contribution of bile secretion to fecal excretion of AMN107 was determined via the comparison to that of intact (uncannulated) rats.

Schedule: Blood samples were collected predose (n=3/time point), and at 0, 0.083 (5 min), 0.25, 0.5, 1, 2, 4, 8, 12, 24, 48, 72, and 96 hr post dose, and urine/feces samples collected for 0-24, 24-48, 48-72, 72-96 and 96-168 hr intervals. Bile samples were collected at 2, 4, 8, 12, 24, 48 and 72 hr.

Analysis: AMN107 plasma levels (LLOQ of 1 ng/mL, upper limit ULOQ of 500 ng/mL), metabolite profiling/structural characterization were analyzed by HPLC/(TOF) MS/MS. The radioactivity was determined by liquid scintillation.

- PK parameters of uncannulated rats:

	Oral (20 mg/kg)		IV (5 mg/kg)	
	Plasma AMN107	Radioactivity	Plasma AMN107	Radioactivity
$AUC_{0-\infty}$	26.1 μg•h/mL	26 μgEq•h/mL	19.3 μg•h/mL	25 μgEq•h/mL
C_{max}	1.74 μg/mL	1.72 μgEq/mL	10.5 μg/mL	10.1 μgEq/mL
T_{max} (hr)	4.0	5	0.083	0.083
Apparent terminal $t_{1/2}$ (h)		25		70
$T_{1/2\alpha}$ (h)	3.8	----	1.5 (83% of $AUC_{0-\infty}$)	----
$T_{1/2\beta}$ (h)	41	----	116 (17% of $AUC_{0-\infty}$)	----
CL (L/h/kg)	----	----	0.26	----
Vss (L/kg)	----	----	7.9	----
Absorption (%)	~26-34	----	Not applicable	----

- Excretion of AMN107 and radioactivity recovery:

	Oral		IV	
Bile duct cannulation	No	Yes	No	Yes
Excretion (AMN107, % dose)				
In urine (0-72 h)	<0.01	---	0.01	----
In feces (0-48 or 72 h)	38.6	30	25.4	9.5
In bile (0-24 h)	----	0.32	----	1.3
Excretion (% dose)				
Total radioactivity recovery	86.3 ± 4.9	83.3 ± 19.9	95.9 ± 1.9	97.3
In urine				
0-24 h	0.90 ± 0.23	1.16 ± 0.51	1.53 ± 0.15	2.83
0-72 h	----	2.71 ± 2.5	----	3.14
0-168 h	1.67 ± 0.50	----	2.51 ± 0.05	----
In feces				
0-24 h	47.9 ± 10.7	26.8 ± 17.6	78.2 ± 12.1	17.7
0-72 h	----	55.2 ± 20.6	----	21.8
0-168 h	84.4 ± 5.3	----	91.3 ± 1.9	----
In bile				
0-24 h	----	23.2 ± 3.8	----	70.9
0-72 h	----	25.4 ± 6.2	----	72.4
Cage wash	0.17 ± 0.09	0.09 ± 0.10	0.21 ± 0.17	----
Absorption (%)	26-34	28	Not applicable	Not applicable

The primary metabolic pathways included:

- Oxidation: methyl-imidazole ring and the pyridinyl-pyrimidine moiety
- Oxidative cleavage: methyl-imidazole ring
- Amide bond hydrolysis

The major metabolites included P20, P13A and P42.1. The proposed metabolic pathway of AMN107 in rats can be found in the figure in Section 2.6.5 (Page 67). The profile of parent drug and metabolites in the circulation is summarized in the table on Page 68. The major

circulating component in the plasma after one single oral dose was AMN107 (84% of total AUC).

DMPK R0500055: Absorption, metabolism, and excretion following a single intravenous or oral dose of [^{14}C]AMN107 in the rabbit

Key study findigs:

- Orally administered AMN107 was absorbed rapidly and excreted through feces.
- Elimination was apparently biphasic.
- Lower oral bioavailability than absorption (% dose) indicated a first-pass effect.
- The major circulating components in the plasma was AMN107 (21% AUC) and P20 (26% AUC).

Study system: Female New Zealand White rabbits

Treatment: [^{14}C]AMN107 (specific activity: 4.99 and 40.5 µCi/mg for oral and IV, respectively) orally (gavage) or intravenously.

Parameters: Blood samples from each rabbit were collected predose, and at 0, 0.083 (5 min), 0.25, 0.5, 1, 2, 4, 6, 8, 12, 24, 48, 72, 96, and 168 hr post dose, and urine/feces samples collected for 0-24, 24-48, 48-72, 72-96 and 96-168 hr intervals.

Analysis: AMN107 plasma levels (LLOQ of 2.5 ng/mL), metabolite profiling/structural characterization were analyzed by HPLC/(TOF) MS/MS. The radioactivity was determined by liquid scintillation.

- PK parameters:

	Oral (30 mg/kg) (n=3)		IV (4 mg/kg) (n=2)	
	Plasma AMN107	Radioactivity	Plasma AMN107	Radioactivity
$AUC_{0-\infty}$	8.73 µg•h/mL	Blood: 72.6 (a) Plasma: 57.2 (a)	5.94 µg•h/mL	Blood: 16.4 (a) Plasma: 15.6 (a)
C_{max}	1.58 µg/mL	Blood: 4.68 (a) Plasma: 5.57 (a)	5.65 µg/mL	Blood: 6.54 (a) Plasma: 8.64 (a)
T_{max} (hr)	1	Blood:1 Plasma: 1.6	0.083	0.083
Terminal $t_{1/2}$ (h)*	10 ± 2.2	Blood: 87± 21 Plasma: 73± 4.5	2	Blood: 133 Plasma: 41
Plasma $t_{1/2\alpha}$ (h)	1.8 ± 0.7	----	0.79 (86% of $AUC_{0-\infty}$)	----
Plasma $t_{1/2\beta}$ (h)	14	----	3 (14% of $AUC_{0-\infty}$)	----
CL (L/h/kg)	----	----	0.68	----
Vss (L/kg)	----	----	0.90	----
Absorption (%)	~49-59	----	Not applicable	----
Bioavailability (%)	20 ± 0.8	----	Not applicable	----

*** Apparent terminal $t_{1/2}$ for radioactivity detection**

(a): AUC and C_{max}: µgEq•h/mL and µgEq/mL, respectively.

- Excretion of AMN107 and radioactivity recovery:

	Oral	IV
Excretion (AMN107, % dose)		
In urine (0-72 h)	Not detected	Not detected
In feces (0-72 h)	35.6	20.5
Excretion (% dose)		
Total radioactivity recovery	Complete (100 ± 3.05)	Complete (106)
In urine		
0-48 h	27.5 ± 3.0	17.6
0-168 h	28.8 ± 3.1	18.2
In feces		
0-72 h	69.2 ± 1.6	86.1
0-168 h	70.9 ± 0.4	87.4
Cage wash	0.26 ± 0.38	0.06

The primary metabolic pathways included:
- Oxidation: methyl-imidazole ring and the pyridinyl-pyrimidine moiety
- Oxidative cleavage and/or hydrolysis of the oxidized methyl-imidazole ring
- Amide bond hydrolysis
- Direct glucuronidation

The major metabolites included P20, P13A and P42.1. The proposed metabolic pathway of AMN107 in rabbits can be found in the figure in Section 2.6.5 (Page 67). The profile of parent drug and metabolites in the circulation is summarized in the table on Page 68. The major circulating component in the plasma after one single oral dose was AMN107 and P20 (21% and 26% of total AUC, respectively).

DMPK R0500294: Absorption, metabolism, and excretion following a single intravenous or oral dose of [^{14}C]AMN107 in monkeys

Key study findings:
- Orally administered AMN107 was absorbed rapidly and excreted mainly via feces.
- Elimination was apparently biphasic.
- The major circulating component in the plasma was AMN107 (54% AUC).

Study system:	Male cynomolgus monkeys
Treatment:	[^{14}C]AMN107 (specific activity: 14.9 and 48 μCi/mg for oral and IV, respectively) orally (gavage) or intravenously.
Schedule:	Blood samples were collected predose (n=3/time point), and at 0, 0.083 (5 min), 0.25, 0.5, 1, 2, 4, 6, 8, 12, 24, 48, 72, 96, and 168 hr post dose, and urine/feces samples collected for 0-24, 24-48, 48-72, 72-96 and 96-168 hr intervals.
Analysis:	AMN107 plasma levels (LLOQ of 2.5 ng/mL), metabolite profiling/structural characterization were analyzed by HPLC/(TOF) MS/MS. The radioactivity was determined by liquid scintillation.

- PK parameters of monkeys:

	Oral (10 mg/kg) (n=3)		IV (3 mg/kg) (n=2)	
	Plasma AMN107	Radioactivity (b)	Plasma AMN107	Radioactivity (b)
$AUC_{0-\infty}$	3.88 µg•h/mL	6.93 (a)	4.77 µg•h/mL	18.3 (a)
C_{max}	0.52 µg/mL	1.02 (a)	6.38 µg/mL	9.01 (a)
T_{max} (hr)	2.7 ± 1.2	3.3± 1.2	0.083	0.083
Apparent terminal $t_{1/2}$ (h)	24 ± 4.5	32± 7.8	2	58
Plasma $t_{1/2\alpha}$ (h)	1.2	----	0.14 (36% of $AUC_{0-\infty}$)	----
Plasma $t_{1/2\beta}$ (h)	21 ± 6.6	----	1.3 (64% of $AUC_{0-\infty}$)	----
CL (L/h/kg)	----	----	0.66	----
Vss (L/kg)	----	----	0.67	----
Absorption (%)	≥ 24	----	Not applicable	----
Bioavailability (%)	24 ± 2.8	----	Not applicable	----

(a): AUC and C_{max}: µgEq•h/mL and µgEq/mL, respectively.
(b): [^{14}C]radioactivity in plasma

Note that the elimination phase of the two-compartment model of plasma AMN107 account for 64% of total AUC.

- Excretion of AMN107 and radioactivity recovery:

	Oral	IV
Excretion (AMN107, % dose)		
In urine (0-72 h)	0.08	Trace
In feces (0-72 h)	57.8	1.36
Excretion (% dose)		
Total radioactivity recovery	96.5 ± 0.85	Complete (102)
In urine		
0-24 h	0.14 ± 0.05	0.29
0-168 h	1.63 ± 1.98	0.81
In feces		
0-72 h	91.0 ± 4.86	6.46
0-168 h	92.8 ± 4.33	91.7
Cage wash	1.98 ± 1.88	9.87

The primary metabolic pathways included:

- Oxidation: methyl-imidazole ring and the pyridinyl-pyrimidine moiety
- Oxidative cleavage and/or hydrolysis of the oxidized methyl-imidazole ring
- Amide bond hydrolysis

The major metabolites included P51 and P35.7. The proposed metabolic pathway of AMN107 in monkeys can be found in the figure in Section 2.6.5 (Page 67). The profile of parent drug and metabolites in the circulation is summarized in the table on Page 68. The major circulating component in the plasma after one single oral dose was AMN107 (54% of total AUC).

2.6.4.4 Distribution

The following two studies were related in terms of study objectives, methods and format of data presentations and thus were reviewed together.

ADME (US) R0300252: *In vitro* blood distribution and binding of ^{3}H-labeled AMN107 to plasma and/or serum proteins in the rat, dog, and human

DMPK R0500654: *In vitro* blood distribution and binding of ^{3}H-labeled AMN107 to plasma proteins in the mouse and monkey

Key study findings:

- AMN107 distribution to plasma was higher than that to blood cells in all species tested. The finding was independent of concentration.
- The plasma protein binding of AMN107 was high (over 97% in all tested species). It was independent of concentration and with no obvious species difference.
- The protein binding in human serum was comparable to plasma, i.e., 99.1% versus 98.4%.

The *in vitro* distribution between red blood cells and plasma, and the *in vitro* plasma protein binding of AMN107 in the mouse (male CD-1 mice), rat (male Wistar-Hannover rats), dog (beagle dogs), monkey (male cynomolgus monkeys), and human (healthy male volunteers) were investigated. AMN107 at concentrations from 0.02-100 μg/mL was incubated with 10 μl of [^{3}H]AMN107 (specific activity 750-757 μCi/mg, final radioactivity of 0.01514 μCi/mL) and 0.5 mL (mouse and monkey) or 1 mL (rat, dog and human) of the following samples: blood, plasma or serum (human only), at 37°C for 30 min. An aliquot (50 μl) of the whole blood sample and plasma sample (after separation of blood cells by centrifugation) was counted to determine the distribution to blood cells. The fraction of drug in blood that was distributed to blood cells (f_{BC}) was calculated as following:

$$f_{BC} = 1 - (1-H)(C_p/C_b) = (C_{bc}/C_b)H$$

H: the hematocrit value, C_p, C_b, C_{bc}: radioactivity measured in plasma, blood and blood cells, respectively.

The plasma and serum protein binding were examined by the ultracentrifugation method: an aliquot of incubate (50 μl) and filtrate (supernatant) were counted by liquid scintillation. Bound fraction was calculated as $(T-C_f)/T$, where T and C_f was the radioactivity in plasma/serum and supernatant, respectively. Another 50 μl aliquot of the supernatant was used for protein analysis.

In vitro [^{3}H]AMN107 blood-to-plasma ratios (mean ± SD)* at 37°C is summarized in the table below:

Concentration (μg/mL)	Mouse	Rat	Dog	Monkey	Human
0.02	0.76**	0.82 ± 0.17	0.80 ± 0.05	0.62 ± 0.05	0.60 ± 0.06
0.1	0.77 ± 0.18	0.72 ± 0.02	0.81 ± 0.08	0.64 ± 0.01	0.70 ± 0.11
1	0.80 ± 0.13	0.81 ± 0.07	0.82 ± 0.13	0.92 ± 0.03	0.70 ± 0.09
10	0.88 ± 0.12	0.83 ± 0.11	0.82 ± 0.06	0.94 ± 0.15	0.69 ± 0.21
100	1.0 ± 0.04	0.77 ± 0.04	0.89 ± 0.03	0.92 ± 0.29	0.70 ± 0.04
Average§	0.84 ± 0.1	0.79 ± 0.09	0.83 ± 0.07	0.81 ± 0.16	0.68 ± 0.11

*** Pooled blood samples of n > 30 for mice, n>3 for rats, and n=3 for dogs, monkeys and humans. Data were obtained from triplicate analyses.**
**** Only two samples, one sample had a technical error.**
§ Average values were presented by the sponsor because there was no clear concentration relationship, if the great variability among analyses (not shown in the table, presented in the Appendix) was taken into consideration. The reviewer concurred.

In vitro [^{3}H]AMN107 distribution into blood cells (f_{BC}, mean ± SD)* at 37°C is summarized in the table below:

Concentration (µg/mL)	Mouse	Rat	Dog	Monkey	Human
0.02	0.18**	0.31 ± 0.14	0.35 ± 0.05	0.07 ± 0.07	0.09 ± 0.12
0.1	0.17 ± 0.23	0.24 ± 0.02	0.36 ± 0.06	0.11 ± 0.01	0.21 ± 0.13
1	0.22 ± 0.13	0.32 ± 0.06	0.36 ± 0.10	0.38 ± 0.02	0.22 ± 0.13
10	0.30 ± 0.10	0.33 ± 0.09	0.37 ± 0.04	0.38 ± 0.09	0.17 ± 0.21
100	0.39 ± 0.02	0.29 ± 0.03	0.41 ± 0.02	0.34 ± 0.21	0.23 ± 0.06
Average§	0.26 ± 0.15	0.30 ± 0.08	0.37 ± 0.06	0.25 ± 0.17	0.18 ± 0.13

In vitro plasma protein binding (%) of [^{3}H]AMN107 (mean ± SD)* at 37°C is summarized in the table below:

Concentration (µg/mL)	Mouse	Rat	Dog	Monkey	Human
0.02	0.979 ± 0.020	0.995 ± 0.001	0.990 ± 0.000	0.996 ± 0.001	0.994 ± 0.000
0.1	0.991 ± 0.001	0.973**	0.988 ± 0.003	0.994 ± 0.001	0.992 ± 0.002
1	0.972 ± 0.017	0.995 ± 0.001	0.981 ± 0.004	0.991 ± 0.002	0.982 ± 0.002
10	0.963 ± 0.025	0.994 ± 0.001	0.985 ± 0.001	0.983 ± 0.006	0.980 ± 0.002
100	0.964 ± 0.020	0.993**	0.966 ± 0.021	0.984 ± 0.006	0.970 ± 0.010
Average§	0.974 ± 0.020	0.991 ± 0.008	0.982 ± 0.012	0.990 ± 0.006	0.984 ± 0.010

**** only two samples due to the protein concentration in one of supernatant samples did not meet the criteria (<50 mg/dl).**

In vitro serum protein binding (%) of [^{3}H]AMN107 in human at 37°C:

Concentration (µg/mL)	Subject 1	Subject 2	Subject 3	Mean ± SD
0.04 (a)	0.994	0.996	0.996	0.996 ± 0.001
100	0.992	0.989	0.981	0.987 ± 0.006
Average				0.991 ± 0.006

(a): The hot stock solution was added twice and the concentration was changed from 0.02 to 0.04 µg/mL.

DMPK R0400674: *In vitro* protein binding of [^{3}H]AMN107 in human albumin and α_1-acid glycoprotein

Key study findings:

- Binding of AMN107 to human AAG was higher than to HSA.
- The extent of binding was not affected by the concentration of AMN107.

[^{3}H]AMN107 spiked AMN107 samples in phosphate buffered saline (PBS, pH 7.4) at concentrations from 0.05 to 10 µg/mL (containing 0.03758 µCi of ^{3}H/mL) were incubated with samples of human serum albumin (HSA, 10 mg/mL and 40 mg/mL) and human α_1-acid

glycoprotein (AAG, 0.3, 1 and 3 mg/mL) at 37°C for 30 min. Binding to HSA and AAG was determined by the ultracentrifugation method (see above). The results are tabulated below:

[^{3}H]AMN107 (µg/mL)	HSA		AAG		
	10 mg/mL	40 mg/mL	0.3 mg/mL	1 mg/mL	3 mg/mL
0.05	0.996 ± 0.000	0.957 ± 0.010	0.933 ± 0.015	0.962 ± 0.004	0.982 ± 0.002
0.2	0.927 ± 0.026	0.926 ± 0.033	0.938 ± 0.013	0.967 ± 0.002	0.984 ± 0.001
1	0.924*	0.932*	0.940 ± 0.005	0.960 ± 0.004	0.985 ± 0.003
5	0.919*	0.927 ± 0.026	0.938 ± 0.020	0.951*	0.983 ± 0.003
10	0.947 ± 0.010	0.926 ± 0.023	0.955 ± 0.022	0.965 ± 0.007	0.981 ± 0.005
Average	0.938 ± 0.024	0.934 ± 0.023	0.941 ± 0.016	0.962 ± 0.015	0.983 ± 0.003

Data was obtained from triplicate analyses and presented as mean ± SD.
*** n=2, due to the contamination of the supernatant**

ADME (US) R0400671: Tissue distribution following an oral dose of [^{14}C]AMN107 in the rat

Key study findings:

- The highest radioactivity concentrations were found in small intestine, uveal tract, liver, adrenal, glandular stomach, and bile.
- At 168 hr postdose, radioactivity was detected in artery, liver, lung, skin, and uveal tract.
- Concentrations in brain and testes were lower than blood, suggesting minimal penetration to these tissues.

Note: the Amendment-1 to this study (**ADME (US) R0400671-1**) was made to correct the legend to Figure 7-2 (Rat#7-48 h (LEH) to Rat#8-168 h (LEH). There were no other changes and the change did not impact the study outcome.

Objective:	The radioactivity tissue distribution was investigated by quantitative whole-body autoradiography (QWBA)
Study system:	Male rats: LEH (Long Evans Hooded, pigmented) and HW (HanWistar, albino)
Treatment:	One oral dose of [^{14}C]-AMN107 (20 mg/kg as free base or 22.1 mg/kg as HCl salt) in the rat. Each rat received 10 mL/kg of the [^{14}C]-AMN107 solution (~148 µCi/kg) via gavage.
Schedule of tests:	QWBA was performed in eight male LEH rats (at 1, 2, 4, 6, 8, 24, 48 and 168 h postdose, n=1/timepoint) and one male HW rat (at 168 H postdose).
Analysis:	The levels of radioactivity in the tissue were determined by [redacted] All radioactivity concentrations were calculated in ngEq/g. The limit of quatification (LOQ) ranged from [redacted] of tissue in this study.

The figure (from the sponsor) depicted the distribution of total radioactivity in blood, tissues and organs following a 20 mg/kg oral dose in the rats:

Figure 7-2 Tissue, organ, and fluid concentrations of total radioactivity following a 20 mg/kg oral dose of [^{14}C]AMN107 in the rat

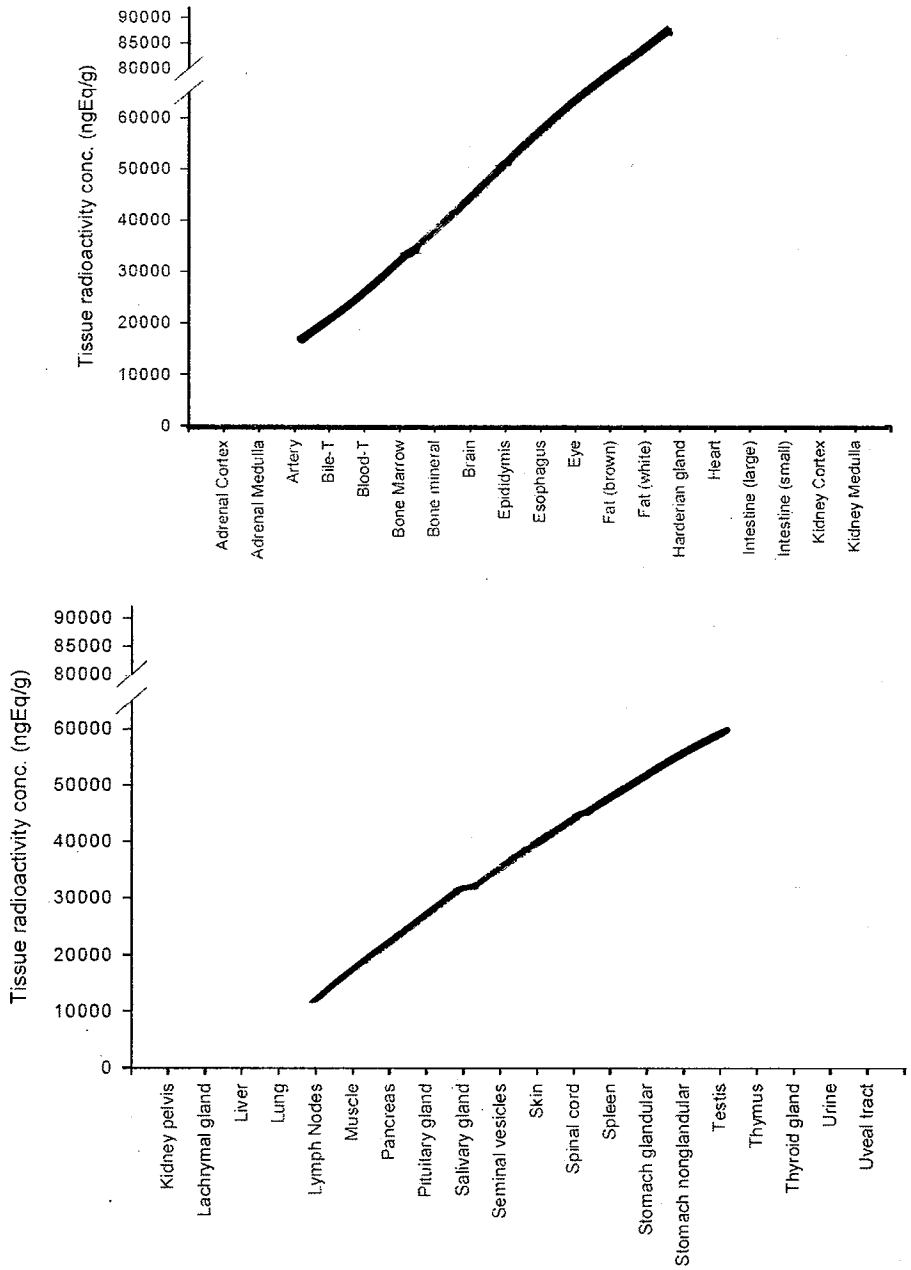

The tissue radioactivity concentrations in fluids, tissues, and organs 1-8 hours after the oral dose were tabulated as follows:

Sample	Radioactivity concentrations (ngEq/g)				
	1 hr	2 hr	4 hr	6 hr	8 hr
Adrenal cortex	7250	13300	8190	10300	4830
Adrenal medulla	4020	7450	NS	3470	2380
Artery (aorta) wall	1410	2880	2140	2800	1330

Sample	Radioactivity concentrations (ngEq/g)				
	1 hr	2 hr	4 hr	6 hr	8 hr
Bile	25400	40800	30600	91900	61700
Blood	804	1550	923	1290	422
Bone marrow	827	1770	1310	2190	694
Brain	45.3	70.2	73.0	74.9	Trace
Epididymis	261	530	493	596	156
Esophagus	773	3590	1550	2200	966
Fat (brown)	1770	3060	2340	3120	1210
Heart	1400	2910	1770	2340	898
Intestine (small)	3980	21800	19200	51500	13800
Kidney cortex	3080	5010	3140	5000	2130
Kidney medulla	2790	4850	3210	4530	2890
Liver	7880	13000	8940	13800	6440
Pancreas	1990	4130	2290	3320	1300
Pituitary	NS	3040	1770	2180	1330
Salivary gland	1400	2890	2050	2680	815
Stomach glandular	18100	4010	2300	2070	5050
Testis	74.7	190	190	TC	192
Thyroid gland	2150	NS	2020	2880	1090
Uveal tract	2870	12300	16500	24900	34000
LOD (ngEq/g)	[redacted]				
LOG (ngEq/g)					

LOD: limit of detection, LOQ: limit of quantification
NS: tissue not sectioned, TC: tissue contaminated
Trace: LOD < concentration < LOQ

ADME (US) R0300234-2: Tissue distribution of radioactivity following a single intravenous dose of [^{3}H]AMN107 in the rat

Key study finding:

- By 24 hr postdose, only thyroid, liver, kidney, lung, skin and uveal tract exhibited concentrations above LOQ
- By 168 hr postdose, only concentrations in liver and uveal tract remained above LOQ.

Objective:	The radioactivity tissue distribution was investigated by quantitative whole-body auoradiography (QWBA)
Study system:	Male rats: LEH (Long Evans Hooded, pigmented) and HW (HanWistar, albino)
Treatment:	One IV dose of [^{3}H]-AMN107 (5 mg/kg) in the rat. Each rat received 2 mL/kg of the [^{3}H]-AMN107 solution (~415 µCi/kg) via a jugular vein catheter.
Schedule of tests:	QWBA was performed in four male LEH rats (0.083, 1, 24, and 168 h postdose, n=1/timepoint) and one male HW rat (at 168 H postdose).
Analysis:	The levels of radioactivity in the tissue were determined by [redacted] All radioactivity concentrations were calculated in ngEq/g. The limit of quantification (LOQ) ranged from [redacted] of tissue in this study.

The figure (from the sponsor) depicted the distribution of total radioactivity in blood, tissues and organs following a 5 mg/kg IV dose in the rats:

Figure 8-2 Tissue, organ, and fluid concentrations of total radioactivity following a single 5 mg/kg intravenous dose of [^{3}H]AMN107 in the rat

Rat #1, 2, 3, and 4 are pigmented (LEH) rats and rat #5 is non-pigmented (HW) rat

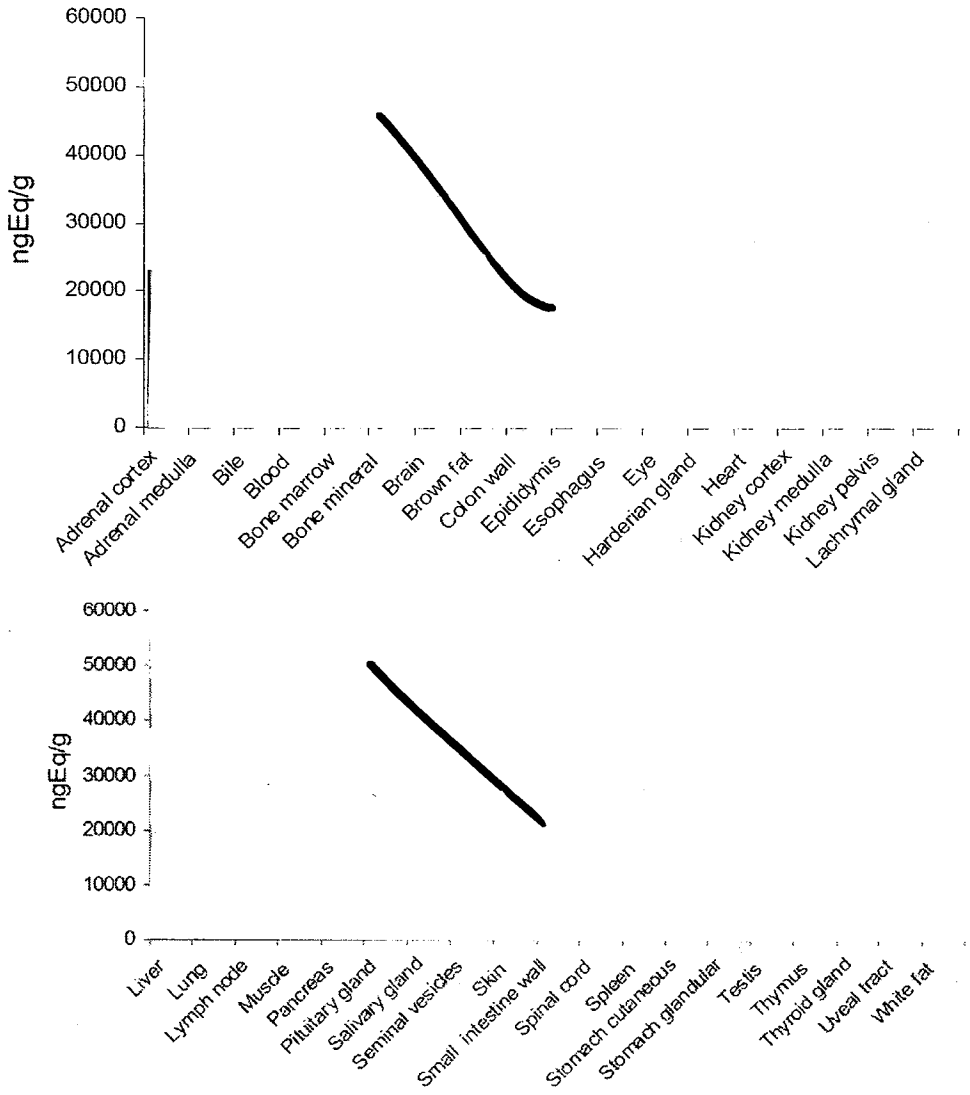

Tissue radioactivity concentrations in fluids, tissues, and organs 5 min (0.083 h) to 1 hour after the IV dose (5 mg/kg) are summarized as following:

Sample	Radioactivity concentrations (ngEq/g)	
	0.083 hr	1 hr
	Rat #1 (LEH)	Rat #2 (LEH)
Adrenal cortex Adrenal medulla Bile		

Sample	Radioactivity concentrations (ngEq/g)	
	0.083 hr	1 hr
	Rat #1 (LEH)	Rat #2 (LEH)
Blood		
Bone marrow		
Brain		
Esophagus		
Heart		
Kidney cortex		
Kidney medulla		
Kidney pelvis		
Liver		
Lung		
Lymph node		
Pancreas		
Salivary gland		
Small intestine		
Spleen		
Stomach glandular		
Testis		
Thyroid gland		
Uveal tract		
LOD (ngEq/g)		
LOG (ngEq/g)		

DMPK R0600047: Tissue distribution of radioactivity following an oral dose of [^{14}C]AMN107 in the pregnant rat

Key study findings: The radioactivity distributed, after a single oral dose, to maternal (liver, kidney, heart, lung, spleen, mammary gland, placenta and uterus) and fetal tissues/organs (blood, brain, and liver).

Objective:	The radioactivity tissue distribution (pregnant rats and fetuses) was investigated by quantitative whole-body auoradiography (QWBA)
Study system:	Eight pregnant Wistar Hannover rats (four females each at gestational Day 10 and Day17)
Treatment:	One oral dose of [^{14}C]-AMN107 (20 mg/kg as free base or 22.1 mg/kg as HCl salt) in the rat. Each rat received 10 mL/kg of the [^{14}C]-AMN107 solution (~289 µCi/kg) via gavage.
Schedule of tests:	QWBA was performed at 1, 3, 6, and 24 h postdose (n=1/timepoint).
Analysis:	The levels of radioactivity in the tissue were determined by [redacted] All radioactivity concentrations were calculated in ngEq/g. The limit of quatification (LOQ) ranged from [redacted] of tissue in this study.

The figure (from the sponsor) depicted the distribution of total radioactivity in maternal and fetal tissues and organs following a 20 mg/kg oral dose in the rats:

Gestation Day 10:

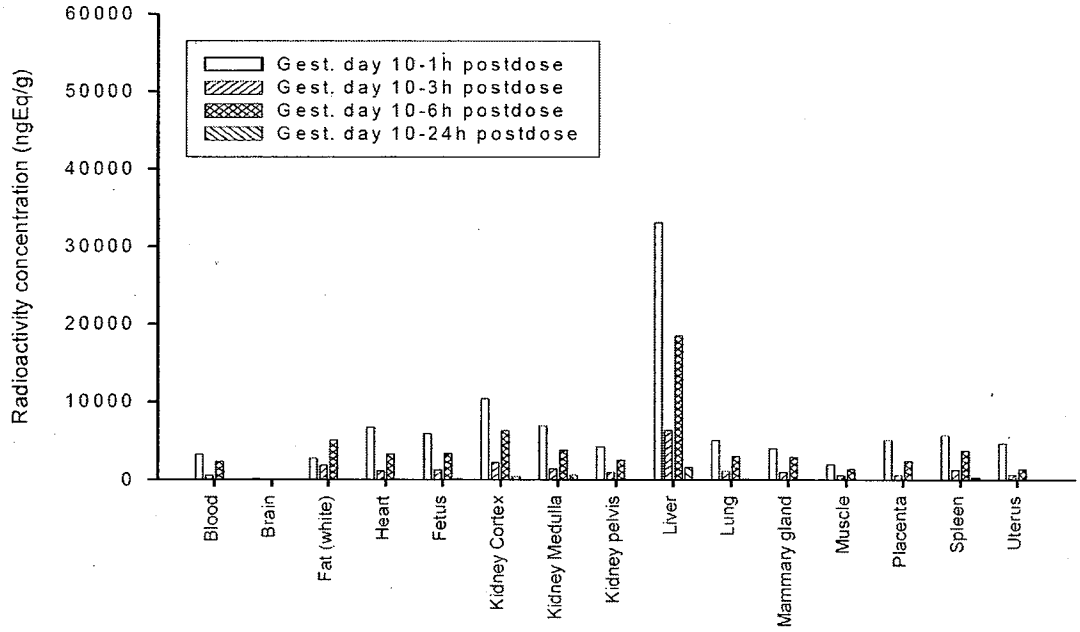

Gestation Day 17:

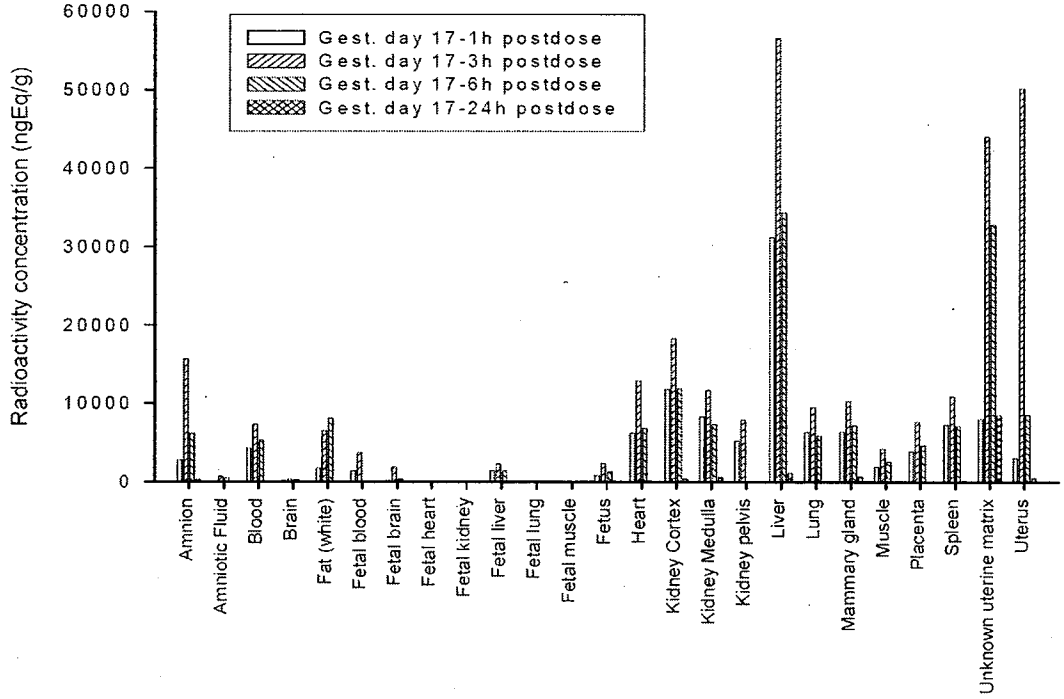

The radioactivity distributed rapidly and reached peaks within 1-3 hours after a single oral dose in many maternal organs (liver, kidney, heart, lung, spleen, mammary gland, placenta and uterus) and in fetus. The maternal distribution patterns were similar on gestation Day 10 and Day 17.

Tissue distribution of radioactivity in the fetus: blood, brain, liver was higher on gestation Day 17 and became detectable, compared to GD 10. On GD17, AMN107 radioactivity in fetal heart, kidney, lung or muscle remained undistinguishable from surrounding tissues and/or background. Thus, AMN107 distribution through blood-brain barrier was low, but it did pass the placenta to reach the fetus.

2.6.4.5 Metabolism

Two *in vitro* studies were reviewed in this section. Additional *in vivo* metabolism data were under Sections 2.6.4.3 and 2.6.4.7. "Absorption". The *in vivo* metabolic pathways were depicted in the figure (from the sponsor) in Section 2.6.5.

ADME (US) R0400853: *In vitro* metabolism of AMN107 by liver S9 fraction isolated from Aroclor-induced rats

Key study findings: The primary metabolites of AMN107 in rat liver S9 fraction were P42.1, P33.1, and P24.5.

The metabolic pathways and the phase 1 metabolites formed during incubation of [^{3}H]AMN107 (specific activity 750 μCi/mg) with Aroclor-induced rat liver S9 fraction (protein concentration 38.2 mg/mL) was investigated. Ten microliters (10 μl) of [^{3}H]AMN107 and S9 fraction (1.9 mg/mL) was incubated at 37°C for 1 hour. AMN107 and its metabolites were analyzed by HPLC with off-line radioactivity detection and metabolite structural characterization was carried out using LC/TOF MS/MS.

The pathway involved in the *in vitro* metabolism of AMN107 in the presence of rat S9 fraction was proposed as the following:

- The primary metabolic reaction: hydroxylation at the methyl benzamide moiety (P42.1).
- Further oxidation of P42.1 to a carboxylic acid, P33.1.
- Oxidation of P33.1 (hydroxylation at the methyl-imidazole moiety) to form P24.5
- The detection of P42.1 and its related metabolites (P24.5 and P33.1) was attributed to the induction of the CYP1A family of enzymes by rat S9 fraction.

ADME (US) R0300235: *In vitro* metabolism of [^{3}H]AMN107 in rat, dog, monkey, human liver slices and human hepatocytes

Key study findings: The following metabolites were commonly found in all species tested: P20, P36, P36.5, P41.6, P42.1, P47 and P50.

The *in vitro* metabolic pathways of [^{3}H]AMN107 (specific activity 750 μCi/mg) was investigated by incubation with rat, dog, monkey, human liver slices and human hepatocytes. [^{3}H]AMN107 at concentrations of 7.5 μM to 14 μM were incubated at 37°C with the liver homogenates and human hepatocytes for 1, 2, 4, 8, 18 and 24 hours. AMN107 and its metabolites were analyzed by HPLC with off-line radioactivity detection and metabolite structural characterization was carried out using LC/TOF MS/MS.

The *in vitro* metabolite profiles of AMN107 in rat, dog, monkey, human liver preparations were complex and qualitative and quantitative differently cross-species. The metabolic reactions, in general, were comparable to those found *in vivo*, e.g., oxidation of the methyl-imidazole ring and the pyridinyl-pyrimidinyl-amino-methyl-benzamide moiety, degradation of the oxidized imidazole, amide hydrolysis, glucuronic acid conjugation with parent compound or metabolites, and various combinations of the above routes. The rat and monkey profiles were most similar to that of human, and dog the least similar. The following metabolites were commonly found in all species tested: P20, P36, P36.5, P41.6, P42.1, P47 and P50.

2.6.4.6 Excretion

Some studies are reviewed under Section 2.6.4.3 "Absorption".

DMPK R0600046: Excretion in milk after a single oral dose of [^{14}C]AMN107 in the rat

Key study findings: Following one single oral dose of [^{14}C]AMN107 to lactating rats, AMN107 and its metabolites were found in the milk, with the plasma AUC:milk AUC ratio of 2.1:1.

The transfer of AMN107 and its metabolites into milk was investigated by administering one single oral dose of [^{14}C]AMN107 (20 mg/kg as free base or 22.1 mg/kg as HCl salt) to lactating rats. Each of the thirteen female rats on Day 7 or 8 post parturition received 10 mL/kg of the [^{14}C]AMN107 solution (232 µCi/kg) via gavage. Milk samples were collected at 1, 2, 4, 8 and 24 hr postdose (n=2-3 at each time point) and blood (plasma) samples were collected from the vena cava of the rat after milking. A 20 µl aliquot of each plasma sample at each time point (with exception at 24 hr: 100 µl) was used for radioactivity analysis and the rest was for metabolite pattern analysis. AMN107 and its metabolites in the plasma and milk were analyzed by HPLC with off-line radioactivity detection and metabolite structural characterization was carried out using LC/TOF MS/MS.

The PK in plasma and milk, indicated as radioactivity concentration was summarized as the following:

	Plasma	Milk
C_{max} (ngEq/mL)	8620	15500 (1:1.8)
$AUC_{0\text{-}24h}$ (ngEq•h/mL)	71900	152000 (1:2.1)
$AUC_{0\text{-}\infty}$ (ngEq•h/mL)	72100	152000 (1:2.1)
T_{max} (hr)	2	4

Numbers in the parentheses represented plasma:milk ratios.

The comparison of the parent drug and metabolite profiles in plasma and milk was tabulated in the tables below:

Plasma:

	AMN107	P20/P40.5	P42.1	P13A	P36	P41.6	P13B	P12	P57
AUC%*	74.5	8.67	3.73	2.82	2.63	2.35	1.85	1.19	0.98
T_{max}	2	4	4	2	4	2	2	2	1

AUC%: $AUC_{0\text{-}24h}$ of parent drug or metabolite/total $AUC_{0\text{-}24h}$

P40.5: a methyl ester artifact of P20 formed from the reaction with methanol in the reconstituting solvent

Milk:

	AMN107	P42.1	P36	P41.6	P43	P50	P57	P47	P13A	P20
AUC%*	52.4	13.5	11.2	11.1	3.69	1.62	1.36	1.00	0.61	0.20
T_{max}	4	4	4	4	8	4	1	2	4	1

The parent drug was the main component in the plasma and milk. The metabolite profile in the plasma and milk were qualitatively and quantitatively different (see two tables above).

According to the sponsor, based on the plasma:milk ratio (1:2.1) in the lactating rats, it is estimated that the maximum amount of AMN107 and its metabolites that a breast-fed infant could be exposed to is 1040 µgEq per day, or 0.26% of a 400 mg adult dose (i.e., ½ of the recommended human dose 400 mg twice a day), if the baby ingesting 1 liter of milk per day. (*Reviewer's note*: The AUC in human after one single oral dose was 11900 ngEq•h/mL in plasma [Page 62, "Pharmacokinetics tabulated summary", this review], or 285600 µgEq•24h/L.
Thus, 1040 µgEq per day/1 liter of milk would be 0.36% of systemic AUC, instead of 0.26%. It is not clear how the sponsor obtained the estimated value of 1040 µgEq per day/1 liter of milk.)

2.6.4.7 Pharmacokinetic drug interactions
ADME (US) R0300236: *In vitro* assessment of cytochrome P450 enzyme inhibition by NVP-AMN107

Key study findings: AMN107 inhibited the following CYP enzymes: 2D6, 2C19, 2C9, 3A4/5 and 2C8

The potential of AMN107 in the inhibition of human cytochrome P450 (CYP) enzyme activity was assessed in pooled human liver microsomes. The following CYP enzyme-selective activities were tested and their probe substrates were also listed (table from the sponsor).

Inhibitory effect of AMN107 on CYP enzyme-selective metabolic reactions

CYP Enzyme	Probe reaction	IC_{50} value[a] (µM)
CYP1A2	phenacetin *O*-deethylation	>100
CYP2C8	paclitaxel 6α-hydroxylation	< 1
CYP2C9	diclofenac 4′-hydroxylation	~ 3
CYP2C19	*S*-mephenytoin 4′-hydroxylation	~ 5
CYP2D6	bufuralol 1′-hydroxylation	~ 7.5
CYP2E1	chlorzoxazone 6-hydroxylation	>100
CYP3A4/5	midazolam 1′-hydroxylation	~ 1
CYP3A4/5	testosterone 6β-hydroxylation	~ 1

[a]AMN107 concentration producing 50% inhibition of probe substrate metabolism.

Under the conditions of the study, AMN107 showed little or no inhibition on CYP1A2 and CYP2E1, but exerted inhibitory effects on the following CYP enzymes: 2D6, 2C19, 2C9,

3A4/5 and 2C8. The inhibition on these CYPs was not time dependent. Thus, AMN107 may inhibit the metabolic clearance/biotransformation of concurrent drugs that involved CYP enzymes mentioned above.

DMPK R0500591: *In vitro* assessment of UGT1A1 inhibition by NVP-AMN107

Key study findings: AMN107 inhibited the UGT1A1 with IC_{50} values at < 1 μM.

The inhibitory effects of AMN107 on human UGT1A1 (uridine diphosphate-glucuronosyltransferase 1A1) were assessed by measuring bilirubin glucuronidataion and estradiol-3-glucuronidation activity in pooled human hepatocytes, liver microsomes (HLM) and membrane fractions prepared from insect cells transfected with a recombinant human UGT1A1 expressing vector. AMN107 induced inhibition of UGT1A1 mediated glucuronidation of bilirubin and β-estradiol with IC_{50} values at < 1 μM. The results are illustrated in the following figures (from the sponsor):

Figure 7-4 Inhibition of [^{3}H]bilirubin glucuronidation activity of human liver microsomes by AMN107

[19-^{3}H]bilirubin was incubated for 15 min at 37°C with human liver microsomes (0.1 mg micrsomal protein·mL^{-1}) in potassium phosphate buffer (100 mM, pH 7.4) containing 5 mM $MgCl_2$, 5 mM saccharolactone, and varying concentrations of AMN107 in the presence of UDPGA (5 mM).

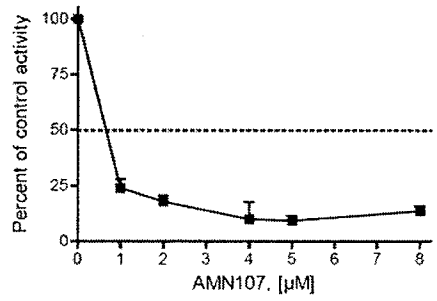

Figure 7-6 Inhibition of [^{3}H]bilirubin glucuronidation activity of insect cell membranes containing recombinant UGT1A1 by AMN107

[19-^{3}H]bilirubin was incubated for 15 min at 37°C with recombinant human UGT1A1 (0.1mg microsomal protein·mL^{-1}) in potassium phosphate buffer (100 mM, pH 7.4) containing 5 mM $MgCl_2$, 5 mM saccharolactone, and varying concentrations of AMN107 in the presence of UDPGA (5 mM).

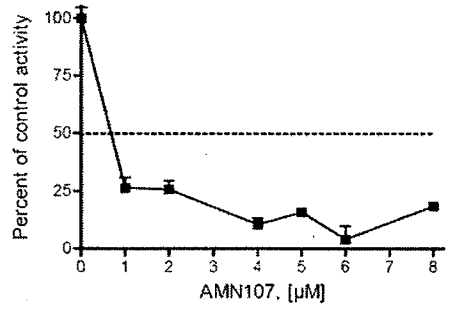

Figure 7-8 Inhibition of estradiol-3-glucuronidation activity of insect cell membranes containing recombinant UGT1A1 by AMN107

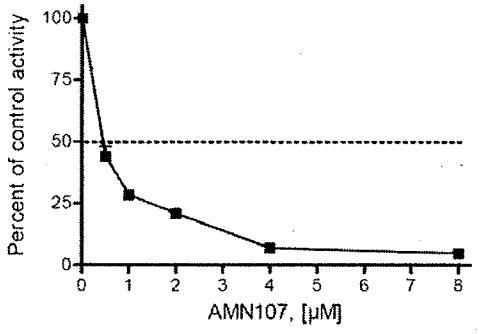

The sponsor suggested that AMN107 may potentially alter the pharmacokinetics of co-medications or endogenous compounds whose metabolism is UGT1A1 dependent.

DMPK R0300237: AMN107: metabolic profile in human liver microsomes, contributions of cytochrome P450s to metabolism and potential for drug-drug interactions

Key study findings: The major CYP isozyme responsible for human hepatic oxidative clearance was CYP3A4.

The metabolic pathway of AMN107 and cytochrome P450s involved in the metabolism were assessed in pooled human liver microsomes (n=38 donors, 17 male and 21 female). The contributions of individual isozymes on AMN107 were determined by the kinetic analysis of the rate of metabolite formation. Also, the effects of specific substrates or inhibitors of individual isozyme on the rate of AMN107 metabolism were further investigated.

Two compounds, with isotope labeled at position of different moiety of AMN107, were used: [^{3}H]AMN107 (specific activity 750 μCi/mg) and [^{14}C]AMN107 (specific activity 100 μCi/mg). AMN107 and its metabolites (in the human liver microsomal preparation) were identified by HPLC analysis and structure characterization were elucidated by HPLC coupled with a TOF MS/MS scans. Metabolism of AMN107 was further characterized by incubation of [^{3}H]AMN107 and individual human recombinant CYP enzymes with the presence of NADPH for 30 min at 37°C. The following CYP450 substrate/inhibitors were used (table excerpted from the sponsor):

Substrate (CYP)	Concentration (μM)	Apparent K_i (μM)
Ketoconazole (3A4)	0-5	0.015-8
Troleandomycin (3A4)	0-100	10-51
Furafylline (1A2)	0-100	3-23
Quinidine (2D6)	0-20	0.027
Paclitaxel (2C8/3A4)	0-20	4-15 (2C8, K_m value) 15 (3A4, K_m value)
Quercetin (2C8/3A4)	0-20	1.3 (2C8) 14 (3A4)
Sulfaphenazole (2C9)	0-200	0.2
S-mephenytoin (2C19)	0-250	58->250

After confirmation of the linear production of metabolites as a function of time and protein (enzyme) concentration, the kinetics of AMN107 metabolism were analyzed by human liver microsomes (using [^{14}C]AMN107 for oxidative metabolites) and human recombinant CYPs.

The main metabolite of AMN107 in human liver microsomes was P41.6, a product of the hydroxylation at the methyl group of the imidazole moiety. Subsequently, the initial hydrozylation was combined with secondary hydroxylation events which produced additional metabolite, i.e., carboxylic acid metabolite P36.5. Trace amounts of a second oxidative metabolite P42.1 (hydroxymethyl benzamide metabolite) were also detected. There were also minor amounts of a direct glucuronide of AMN107, P22, found in the prolonged incubations with high microsomal protein concentration. The major CYP isozyme responsible for hepatic oxidative clearance was CYP3A4. Other CYPs may also play a minor role in catalyzing the oxidation of AMN107, such as CYP2C8 and 1A2. Although CYP2J2 was able to catalyze AMN107 metabolism *in vitro*, calculation of scaled contribution of this CYP isozyme *in vivo* was not possible, due to its low expression levels in the human liver.

The steady-state kinetic parameters of AMN107 metabolism by CYP3A4 were estimated as: K_m 1.8 μM, V_{max} 15.5 nmol•min^{-1}•nmol P450^{-1}, where V_{max} is maximum velocity catalyzed by a fixed enzyme concentration and K_m is the substrate concentration which gives ½ V_{max}. The predicted contribution of CYP3A4 to AMN107 oxidative clearance (CL_{int}: intrinsic clearance, V_{max}/K_m) was 16 mL•h^{-1}•mg protein^{-1} which was similar to the CL_{int} in human liver microsomes. The K_m for other CYPs was under 5 μM, with V_{max} below 2 nmol•min^{-1}•nmol P450^{-1}. The IC_{50} values of the inhibitors were shown in the table below (from the sponsor):

Table 6-4 Estimated IC_{50} values for inhibition of AMN107 metabolism

Inhibitor/substrate (P450)	Inhibitor concentration range (μM)	IC_{50} (μM)	% activity of control at maximum inhibition
Ketoconazole (CYP3A4)	0-5	0.012 (P41.6) 0.013 (P42.1)	2.0 (P41.6) 3.1 (P42.1)
Troleandomycin (CYP3A4)	0-100	1.2 (P41.6) 1.7 (P42.1)	1.7 (P41.6) 18.0 (P42.1)
Quercetin (CYP2C8/3A4)	0-20	>20	73
Paciltaxel (CYP2C8/3A4)	0-20	>20	77
Furafylline (CYP1A2)	0-100	> 100	73 (P41.6) 82 (P42.1)
Quinidine (CYP2D6)	0-20	> 20	100
Sulfaphenazole (CYP2C9)	0-200	> 200	100
S-mephenytoin (CYP2C19)	0-250	> 250	77 (P41.6) 72 (P42.1)

DMPK R0400672: Evaluation of AMN107 as an inducer of cytochrome P450 enzymes drug transporters in human hepatocytes

Key study findings: AMN107 induced the following CYP enzymes: 2B6, 2C8, 2C9, 3A4, and 1A2, and also induced UGT1A1.

The potential of AMN107 in the induction of human cytochrome P450 (CYP) enzymes, UDP-glucuronosyl transferase (UGT) 1A1, ABCB1 (Pgp), and ABCC2 (MPR2) mRNA and CYP1A2, 2B6, 2C8, 2C9, 2C19 and 3A activity was assessed in primary human hepatocytes of three donors after 72 hour of treatment. The mRNA quantification was performed by real-time PCR using the Comparative C_T method, based on the similar amplification efficiencies of the target (P450 enzymes, UGT1A1, ABCB1 or ABCC2) and endogenous primers/probes. CYP probe substrate metabolism was determined by quantitative LC-MS/MS analysis. The table below (from the sponsor) listed the probe substrates and the concentrations used which were above the literature reported K_m.

Table 2-2 Probe substrate concentrations

Probe substrate (solvent)	P450 Enzyme	Concentration (μM)	Literature K_m value (μM)
Phenacetin (0.2% DMSO)	CYP1A2	200	47.0 (HLM) 16.7 (recombinant CYP1A2)
Bupropion (Water)	CYP2B6	500 (Liver 1 and Liver 2) 400 (Liver 3)	81.7 (HLM) 66.8 (recombinant CYP2B6)
Amodiaquine (0.2% DMSO)	CYP2C8	50 (Liver 1 and Liver 2) 100 (Liver 3)	1.89 (HLM) 0.728 (recombinant CYP2C8)
Diclofenac (0.2% DMSO)	CYP2C9	100	4.04 (HLM) 0.589 (recombinant CYP2C9)
S-Mephenytoin (0.2% DMSO)	CYP2C19	200	57.2 (HLM) 17.3 (recombinant CYP2C19)
Midazolam (0.2% DMSO)	CYP3A	100	2.27 (HLM) 0.622 (recombinant CYP3A4) 1.53 (recombinant CYP3A5)

HLM: human liver microsomes.

Conclusion:

- In duction of CYP enzyme activity:
  - AMN107 treatment (up to 10 μM) induced CYP2B6, 2C8 and 2C9 activities after 72 hours above 2 fold of the vehicle control in the primary human hepatocytes. The induction was considered biologically meaningful under the *in vitro* setting, because the induction levels were within 40% of the positive controls.
  - AMN107 induction of enzyme activity of CYP1A2, 2C19 and 3A4 was below 40% of the positive control, although the induction of CYP3A4 and 1A2 was approximately 2 fold of the vehicle control.
  - The induction of CYP3A4 activity may be underestimated, taking the consideration that AMN107 also inhibited CYP3A4 activity.
- Induction of CYP enzyme mRNA:
  - AMN 107 induced increases in mRNA levels of CYP2B6 and CYP3A5 were within 40% of positive control RIF, but below 40% of another positive control PB.
  - AMN107 induced mRNA elevation of CYP1A1, 1A2 and 3A4 was below 40% of the positive control.
  - AMN107 did not induce mRNA of CYP2C8, 2C9 and 2C19.
  - AMN107 induced UGT1A1 mRNA less than 2 fold (average of three donors) and the levels were approximately within 40% of the positive control.
  - AMN107, up to 10 μM, did not induce ABCB1 and ABCC mRNA.

ADME (US) R0400241: The potential of AMN107 to inhibit P-glycoprotein in cells determined by flow cytometry

Key study findings: AMN107 inhibited P-glycoprotein mediated Rhodamine 123 efflux with an IC_{50} of 1.7 μM.

The potential of AMN107 to inhibit P-glycoprotein (Pgp, MDR-1, ABCB-1) was assessed by measuring Pgp mediated efflux of Rhodamine 123 (Rho123) in cells which over-expressed Pgp using flow cytometry. The passive efflux of Rho123 was inhibited by AMN107 (0.1-50 μM) concentration-dependently with an IC_{50} of 1.7 μM. The IC_{50} was comparable to that of the positive control cyclosporine A.

2.6.4.8 Other Pharmacokinetic Studies

No studies were reviewed.

2.6.4.9 Discussion and Conclusions

Orally administered AMN107 was rapidly absorbed. Detectable serum levels of AMN107 were found 0.5 hr after administration as both single and repeated dosing. T_{max}'s were from 0.5 hr (mouse) to 3.5 hr (human, Clinical Study CAMN107A2104) after single dosing, and ~2 to 6 hr in the rat, dog, and monkey after repeated administration. The bioavailability was 43%, 34%, 20%, 24%, and 30%, in mouse, rat, rabbit, monkey, and human (Clinical Study CAMN107A2104), respectively. The plasma protein binding of AMN107 was high (over 97% in all species tested, with no species difference) and was independent of AMN107 concentrations. AMN107 distributed to plasma higher than that to blood cells. In human, the

protein binding in serum was comparable to that in plasma. Binding of AMN107 to human α_1-acid glycoprotein was higher than that to human serum albumin.

A single oral dose of isotope-labeled AMN107 was broadly distributed, with uveal tract, small intestine, glandular stomach, liver, and adrenal as organs of highest radioactivity concentrations. A great amount of radioactivity was found in bile, indicating the contribution of biliary excretion to fecal elimination of AMN107. The high radioactivity trapped in the GI and bile also indicated that the isotope-labeled AMN107 might not be well absorbed under the conditions of the studies. AMN107 apparently binds to melanin, as evidenced by the high distribution to uveal duct of the LEH (Long Evans Hooded) pigmented rats but not the HW (Han Wistar) albino rats. There was little or no findings of radioactivity in the brain or testis, but AMN107 did cross the placenta to enter the fetus, with detectable radioactivity concentrations found in fetal blood, brain and liver. Radioactivity concentrations were also found in milk after a single oral dose to lactating rats, with the plasma:milk ratio of approximately 1:2. It was noted that the parent drug was the main component in both plasma and milk; however, the metabolite profiles were qualitatively and quantitatively different. According to the sponsor, based on the plasma:milk ratio in the lactating rats, it is estimated that the maximum amount of AMN107 and its metabolites that a breast-fed infant could be exposed to is 0.36% of a 400 mg adult dose (recommended human dose 400 mg twice a day), if the baby ingesting 1 liter of milk per day.

In general, the *in vitro* metabolic pathways of AMN107 were comparable to that *in vivo*. The primary metabolic reactions included hydroxylation of the methyl groups on the methyl-imidazole ring, oxidation of the methyl-imidazole ring and the pyridinyl-pyrimidinyl-amino-methyl-benzamide moiety, and amide hydrolysis. Secondary metabolic pathways were similar in all species tested, and included further degradation of the oxidized imidazole, glucuronic acid conjugation with parent compound or metabolites, and various combinations of the above routes. The commonly found metabolites in rat, dog, monkey and human were P20, P36, P36.5, P41.6, P42.1, P47 and P50. The rat and monkey profiles were most similar to that of human, and that in dog was the least. One of the major metabolites in human, P36.5, was not found in plasma of mouse, rat and rabbit; and it was not found in urine or feces of mouse and rat, only trace in rabbit and monkey. P42.1 related metabolites P24.5 and P33.1, not detected in most of the *in vivo* studies, were enriched in the *in vitro* rat liver S9 fraction because the induction of CYP1A family of enzymes.

Cytochrome P450 (CYP) 3A4 was the main CYP isozyme responsible for hepatic oxidative clearance of AMN107. Other CYPs, such as CYP2C8 and 1A2, may also play minor roles. In *in vitro* studies, AMN107 inhibited the following CYP enzymes: 2D6, 2C19, 2C9, 3A4/5 and 2C8, and UGT1A1 as well as P-glycopreotein mediated efflux. AMN107, on the other hand, induced activity of the following CYPs: 2B6, 2C8, 2C9, and 3A4. It also induced the mRNA expression of the following CYPs: 2B6, 3A4/5, 1A1, and 1A2, as well as UGT1A1. Thus, AMN107 may have drug-drug interaction with concurrent drugs whose biotransformation is mediated through these CYP enzymes, UGT1A1 or P-glycoproteins. Elevated blood bilirubin levels observed in patients are related to AMN107-induced inhibition of UGT1A1 mediated glucuronidation of bilirubin.

AMN107 was eliminated mainly through extensive metabolism as summarized above, and excreted mainly via feces. Following a single oral dose, the unchanged AMN107 excreted in feces (0-48 hr or 0-72 hr) was (as % dose): 18.3, 38.6, 35.6, and 57.8% for mouse, rat, rabbit and monkey, respectively. The radioactivity recovery in feces following one oral dose of AMN107 was (as % dose, 0-168 hr): approximately 92, 84, 71, and 93% for mouse, rat, rabbit, and monkey, respectively. The elimination of AMN107 exhibited a biphasic pattern with a prolonged $t_{1/2\beta}$ in rats. In rabbits and monkeys, the elimination was also apparently biphasic, but the $t_{1/2\beta}$ was shorter than that found in rats. The $t_{1/2\beta}$ was comparable in these two species.

Based on approximately 2 fold increase of AUC at the end of repeated administration, regardless of treatment length, it appeared that AMN107 accumulated in monkeys (at all doses tested) and dogs (at higher doses). The accumulation of AMN107 was not consistent through the dose range used in rats. The C_{max} and AUC values increased with doses, and generally were dose-proportionally in rats. However, inconsistent findings were noted in the 4 and 26 week studies in rats. The TK results in Study #0370146 (4 week study) on Day 1 were comparable to those of Study #0580158 (26 week study) (see table below). However, dose normalized AUC elevated on Day 28 in the 4 week study, a finding not shared in the 26 week study. The C_{max} and AUC were less proportionally in dogs and monkeys. According to the sponsor, in clinical trial CAMN107A2101, the C_{max} and AUC values increased also in a less proportional fashion with the dose higher than 400 mg once daily. The obvious gender difference in AMN107 exposure seen in rats, with AUC values higher in females than in males, may be of little clinical relevance, because it was not observed in other species.

2.6.4.10 Tables and figures to include comparative TK summary

The following studies are reviewed in the Toxicology section (Section 2.6.6), including repeat-dose toxicity (Section 2.6.6.3) and reproductive and developmental toxicology (Section 2.6.6.6) studies. These studies are: in rats: Study #0570152- An oral (gavage) fertility and early embryonic development study in rats, #0570057- An oral embryo-fetal development study in rats, #0370147- 4-week oral (gavage) toxicity study in rats with a 4-week recovery period, and #0580158- A 26-week oral (gavage) toxicity study in rats with a 4-week recovery period; in rabbits: #0570058- An oral embryo-fetal development study in rabbits; in dogs: #0370147- 4-week oral (gavage) toxicity study in dogs with a 4-week recovery period; and in monkeys: #0580157- A 39-week oral (gavage) toxicity study incynomolgus monkeys with a 4-week recovery period. See respective sections for reviews.

Species (Duration)	Dose		Sex	C_{max} (ng/mL)		AUC (ng•h/mL)		Dose normalized C_{max}		Dose normalized AUC		Ratio of animal to human exposure	
	(mg/kg)	(mg/m^2)		Day 1	End of Study	Day 1	End of Study	Day 1	End of Study	Day 1	End of Study	C_{max}	AUC
Rats (14 day)	20	120	M	2400	2400	21000	31000	120	120	1050	1550	1.06	0.86
			F	5300	4900	61000	58000	265	245	3050	2900	2.17	1.61
	60	360	M	4700	7200	48000	99000	78	120	800	1650	3.19	2.75
			F	7000	9100	110000	125000	117	152	1833	2083	4.03	3.47
	180	1080	M	6800	12000	97000	162000	38	67	539	900	5.31	4.5
			F	9400	16900	194000	238000	52	94	1078	1322	7.48	6.61
Rats (GD 6-17)	10	60	F		2600		30400		260		3040	1.15	0.84
	30	180	F		5300		72700		177		2423	2.35	2.02
	100	600	F		14600		204000		146		2040	6.46	5.67
Rat (28 day)	6	36	M	1092	1158	6240	6900	182	193	1040	1150	0.51	0.19
			F	1512	1368	12720	11220	252	228	2120	1870	0.61	0.31
	20	120	M	3660	4000	44400	21000	183	121	2220	1050	1.77	0.58
			F	2420	3200	34860	46200	200	160	1740	2310	1.42	1.28
	60	360	M	3870	9240	52080	120000	64.5	154	868	2000	4.09	3.33
			F	4020	13200	60000	187200	67.0	220	1000	3120	5.84	5.2
Rat (26 week)	6	36	M	722	1590	3960	9200	120	265	660	1530	0.70	0.26
			F	1200	2370	6870	15300	200	395	1150	2550	1.05	0.43
	20	120	M	2710	2770	21400	29200	136	139	1070	1460	1.23	0.81
			F	3520	12100	29800	146000	176	605	1490	7300	5.35	4.06
	60	360	M	3890	5840	45700	80200	64.8	97.3	762	1340	2.58	2.23
			F	8830	11200	64200	61842	147	187	1070	1030	4.96	1.72

Rabbits (GD 7-17)	30	360	F		194		2190		6.5		73	0.09	0.06
	100	1200	F		494		5980		4.9		60	0.22	0.17
	300	3600	F		1100		17100		3.7		57	0.49	0.48
Dog (28 day)	5	100	M	280	370	1070	1560	56.0	74.0	214	312	0.16	0.04
			F	357	296	2400	1680	71.4	59.2	480	356	0.13	0.05
	15	300	M	582	1241	5685	11505	38.8	82.7	379	767	0.55	0.32
			F	662	983	3570	5625	44.1	65.5	238	375	0.43	0.16
	45	900	M	446.0	648	3092	3879	9.91	14.4	68.7	86.2	0.29	0.11
			F	878	2039	6300	25700	19.5	45.3	140	571	0.90	0.07
Monkey (39 week)	30	360	M	340	632	5530	9770	11.3	21.1	120	326	0.28	0.27
			F	419	756	10100	11600	14	25.2	184	387	0.33	0.32
	200	2400	M	728	1370	18000	19900	3.6	6.9	41.2	99.5	0.61	0.55
			F	742	965	12100	14900	3.7	4.8	39.4	74.5	0.43	0.41
	600	7200	M	855	1630	17900	26200	1.4	2.7	16	43.7	0.72	0.73
			F	924	1830	25300	24400	1.5	3.1	17.7	40.7	0.81	0.68
Human* (15 day)	9.5** (16)	351.5 (592)	M/F	----	2260	----	36000	----	237.9 (141.3)	----	3789.5 (2250)	Not Applicable	Not Applicable

*** Clinical trial #CAMN107A2101Ph1**

**** At dose of 400 mg, twice daily, or 800 mg total daily dose, with a mean body weight of 84.2 kg (n=17). If based on a theoretical body weight of 50 kg, the dose was 16 mg/kg.**

2.6.5 PHARMACOKINETICS TABULATED SUMMARY

Summary of ADME studies:

- Absorption:

Total radioactivity concentrations (C_{max} and AUC) in blood and plasma following single oral doses of radiolabeled AMN107:

	Dose (mg/kg)	C_{max} (µgEq/mL)		$AUC_{0-\infty}$ (µgEq•h/mL)		Dose normalized C_{max}		Dose normalized AUC	
		Blood	Plasma	Blood	Plasma	Blood	Plasma	blood	Plasma
Mouse	25	10.5	15.1	46.7	69.7	0.42	0.60	1.87	2.79
Rat	20	1.37	1.72	21.5	26	0.068	0.086	1.08	1.3
Rabbit	30	4.68	5.57	72.6	57.2	0.16	0.19	2.42	1.91
Monkey	10	0.61	1.02	4.09	6.93	0.061	0.10	0.41	0.69
Human	5.48 (8)*	---	0.62	---	11.9	---	0.11	---	2.17

Note: the data of humans were not reviewed (Study CAMN107A2104). The table was adapted from sponsor's Table 3-2 in PK written summary (Module 3 Summary: 2.6 nonclinical summary: summary\nonclinical_overview.pdf)

Other PK parameters following single oral and IV administrations:

	Oral				IV		
	Dose (mg/kg)	BA (%)	T_{max} (h)**	Terminal $t_{1/2}$ (h)	Dose (mg/kg)	CL (L/h/kg)	Vss (L/kg)
Mouse	25	43	0.9	0.9	10	0.30	0.52
Rat	20	34	4.0	41	5	0.26	7.9
Rabbit	30	20	1	10	4	0.68	0.90
Monkey	10	24	2.7	24	3	0.66	0.67
Human	5.48 (8)*	~30	3.5	16.5	----	----	----

*** Based a 400 mg dose and mean body weight of 73 kg (50 kg).**
**** AMN107 in plasma**

- Metabolism:

The following figure and tables were excerpted from sponsor (Module 3 Summary: 2.6 nonclinical summary: summary\nonclinical_overview.pdf).

✧ Major metabolites of AMN107 in humans included P36, P36.5, P41.6 and P42.1.

Table 5-2 Dose normalized systemic exposure of species in ADME studies to human metabolites of nilotinib

Plasma exposure after oral dosing to human serum metabolites based on ADME results[a]					
Metabolite[b]	Mouse (25 mg/kg)	Rat (20 mg/kg)	Rabbit (30 mg/kg)	Monkey (10 mg/kg)	Human (5.48 mg/kg)
Dose normalized $AUC_{0\text{-}last}$ (ngEq•h/mL / mg/kg)[c]					
P36	18.0 (0-12 h)	30.9 (0-24 h)	18.8 (0-24 h)	-	15.1 (0-48 h)
P36.5	-[d]	-	-	7.3 (0-24 h)	143 (0-48 h)
P41.6	12.6 (0-12 h)	24.8 (0-24 h)	7.80 (0-24 h)	10.7 (0-24 h)	85.9 (0-48 h)
P42.1	60.4 (0-12 h)	45.5 (0-24 h)	42.0 (0-24 h)	22.1 (0-24 h)	33.9 (0-48 h)
Dose normalized C_{max} (ngEq/mL / mg/kg)					
P36	4.28	4.55	4.70	-	7.30
P36.5	-	-	-	1.70	16.2
P41.6	3.52	2.30	2.53	1.80	10.9
P42.1	14.2	5.05	8.27	2.30	5.11
References	Table 2.6.5.9A, [R0500054]	Table 2.6.5.9C, [R0300234-1]	Table 2.6.5.9E, [R0500055]	Table 2.6.5.9G, [R0500294]	Table 2.6.5.9I, [CAMN107A2104]

[a] The measured AUC and C_{max} values were obtained from the ADME studies listed in references
[b] See figure 5-2 for structures
[c] Time interval for AUC shown in parentheses
[d] Not detected or not quantifiable

- Metabolites of AMN107: cross species comparison:
  - Metabolic pathways for AMN107 in all species:

Figure 5-1 Metabolic pathways for nilotinib in all species

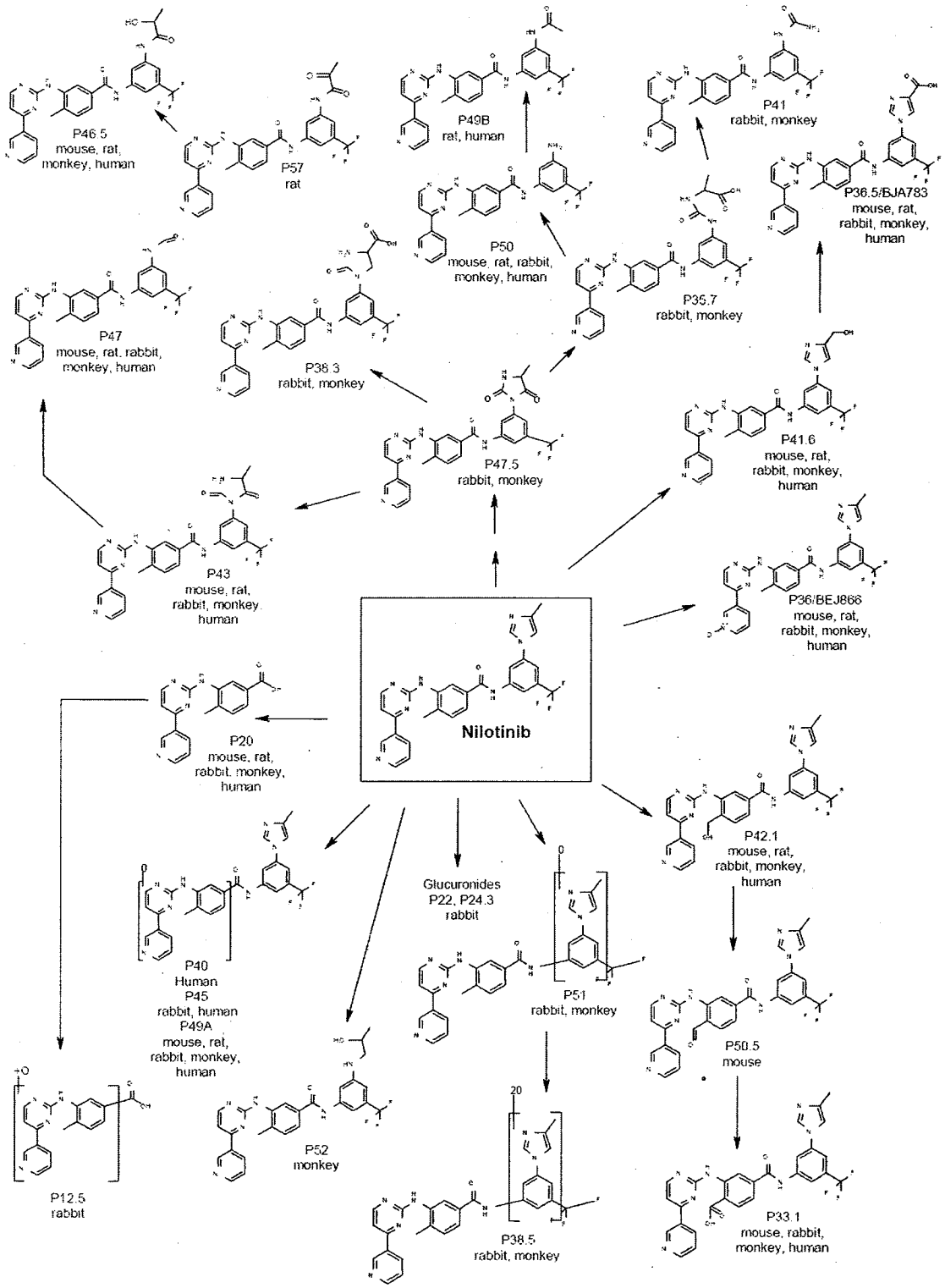

➢ Plasma AUC% of unchanged AMN107 and metabolite:

Table 5-3 Plasma AUC% of nilotinib and circulating metabolites after an oral radiolabeled dose in various species

	AUC % of nilotinib and circulating metabolite				
Metabolite[a]	Mouse (25 mg/kg)	Rat (20 mg/kg)	Rabbit (30 mg/kg)	Monkey (10 mg/kg)	Human (5.48 mg/kg)
P12	-[b]	-	4.2	-	-
P12.5/P13A[c]	6.0	3.2	16	-	-
P13B	0.92	1.0	9.9	-	-
P20	4.2	0.99	26	1.4	-
P20.9	0.51	-	-	-	-
P24.3/P24.4[d]	-	-	1.7	-	-
P27.2	0.22	-	-	-	-
P29.1	-	-	-	1.4	-
P36	0.62	2.2	1.4	-	0.51
P36.5	-	-	-	1.2	6.1
P35.7	-	-	-	4.8	-
P38.1	-	-	4.4	-	-
P38.3/P38.5/P38.6[d]	-	-	2.3	3.9	-
P39.8	0.98	-	-	-	-
P41	-	-	-	0.78	-
P41.6	0.43	1.8	0.60	1.8	4.7
P42.1	2.1	3.3	3.2	3.6	1.3
P45.2	-	-	-	1.7	-
P47	-	0.39	-	-	-
P47.5	-	-	2.1	-	-
P49A	1.3	-	-	-	-
P50	1.10	0.55	-	-	-
P50.5	0.75	-	-	-	-
P51	-	-	1.5	18	-
nilotinib	80	84	21	54	88
P57	-	0.63	-	-	-
References	Table 2.6.5.9A, [R0500054]	Table 2.6.5.9C, [R0300234-1]	Table 2.6.5.9E, [R0500055]	Table 2.6.5.9G, [R0500294]	Table 2.6.5.9I, [CAMN107A2104]

[a] See figure 5-2 for structures

[b] Not detected or not quantifiable

[c] Metabolite 12.5 was only detected in rabbit where it was poorly resolved chromatographically from P13A

[d] Components not chromatographically well-resolved

➢ Unchanged AMN107 and metabolites in urine:

Table 5-4 Metabolites of nilotinib in urine after a single oral radiolabeled dose

	Percent of dose				
Metabolite[a]	Mouse (25 mg/kg) (0-48h)	Rat (20 mg/kg) (0-48h)	Rabbit (30 mg/kg) (0-72h)	Monkey (10 mg/kg) (0-72h)	Human (5.48 mg/kg) (0-144h)
P10A/P10B[b]	-[c]	-	0.68	-	-
P11/P11.4[b]	-	-	1.5	-	-
P11.8/P11.9[b]	-	-	0.47	-	-
P12	-	-	5.0	-	-
P12.5/P13A[d]	0.27	0.23	8.8	0.55	-
P13B	-	0.07	5.2	-	-
P15	-	0.11	-	-	-
P19	-	-	0.03	-	-
P20	4.6	0.34	5.1	0.28	-
P22	-	-	0.03	-	-
P24.3/P24.4[b]	-	-	0.02	-	-
P32.2	-	-	-	0.01	-
P35.7	-	-	-	0.02	-
P36.5/P38.3/P38.5/P38.6[b]	-	-	Trace of P36.5	0.04	-
P41.6	-	-	-	0.01	-
P42.1	-	-	-	Trace	-
P47.5	-	-	-	0.01	-
nilotinib	-	<0.01	-	0.08	-
References	Table 2.6.5.9A, [R0500054]	Table 2.6.5.9C, [R0300234-1]	Table 2.6.5.9E, [R0500055]	Table 2.6.5.9G, [R0500294]	Table 2.6.5.9J, [CAMN107A2104]

[a] See figure 5-2 for structures

[b] Components not chromatographically well-resolved

[c] Not detected or not quantifiable

[d] Metabolite P12.5 was only detected in rabbit where it was poorly resolved chromatographically from P13A

➢ Unchanged AMN107 and metabolites in feces:

Table 5-5 Metabolites of nilotinib in feces after a single oral radiolabeled dose

	Percent of dose				
Metabolite[a]	Mouse (25 mg/kg) (0-48h)	Rat (20 mg/kg) (0-48h)	Rabbit (30 mg/kg) (0-72h)	Monkey (10 mg/kg) (0-72h)	Human (5.48 mg/kg) (0-144h)
P12.5/P13A[b]	0.32	-[c]	trace	-	-
P19	-	-	0.43	-	-
P20	2.93	0.45	1.16	-	0.18
P24.3/P24.4[d]	-	-	0.53	-	-
P24.5	0.78	-	-	-	-
P25.6	1.89	-	-	-	1.12
P25.8	-	-	-	0.49	-
P26.6	-	-	-	0.34	-
P28.6	-	-	-	0.74	-
P31	-	1.01	-	-	0.87
P31A	4.31	-	-	-	-
P31.2	-	-	-	1.07	-
P32.2	-	-	-	0.90	-
P32.5	1.60	0.70	-	-	-
P33.1/P33.4[e]	3.16	-	1.02	-	-
P35.6/P35.7[f]	-	-	1.47	3.02	-
P36	1.41	1.36	0.73	-	-
P36.5	5.52	2.71	-	-	-
P36/P36.5[g]	-	-	-	-	8.08
P37	-	2.08	-	-	-
P37.5	-	0.79	-	-	-
P38	-	-	-	-	0.62
P36.5/P38.3/P38.5/P38.6[h]	-	-	4.21	7.56	-
P40	-	-	-	-	1.2
P41.6	12.3	13.2	4.31	8.04	3.97
P42.1	27.2	9.33	4.74	1.79	1.32
P43	3.16	2.80	0.56	0.39	0.27
P45	-	-	0.35	-	-
P45.2	-	-	-	0.12	-
P45.5	-	-	-	0.22	-
P46.5	0.96	0.84	-	-	-
P47/P47.5[i]	0.73	0.98	3.14	1.43	1.49
P49A/P49B[j]	0.60	1.19	0.80	0.47	1.05
P50	0.81	1.59	0.95	1.03	1.36
P51	-	-	1.95	3.16	-
nilotinib	18.3	38.6	35.6	57.8	68.5
P57	-	0.41	-	-	-

- Excretion: table excerpted from sponsor.

Table 6-1 Excretion of nilotinib and total radioactivity following a single dose of radiolabeled nilotinib

			Amount Excreted (% of Dose)					
			Urine			Feces		
			Radioactivity		Nilotinib	Radioactivity		Nilotinib
Species	Dose (mg/kg)	Dose Route	0-24 h	0-168 h	0-72 h	0-24 h	0-168 h	0-72h
Mouse[a]	10	i.v.	7.36	7.87	-[c]	73.1	76.8	3.15[f]
	25	p.o.	5.44	5.89	-[c]	85.9	91.8	18.3[f]
Rat[b]	5	i.v.	1.53	2.51	0.01	78.2	93.1	25.4[f]
	20	p.o.	0.903	1.67	<0.01	47.9	84.4	38.6[f]
Rabbit[d]	4	i.v.	15.6	18.2	-[c]	44.7	87.4	20.5
	30	p.o.	22.1	28.8	-[c]	30.8	70.9	35.6
Monkey[e]	3	i.v.	0.294	0.814	-[c]	42.1	91.7	1.36
	10	p.o.	0.144	1.63	0.08	22.7	92.8	57.8
Human[g]	5.48	p.o.	-[c]	-[c]	-[c]	-[c]	93.5	68.5

[a] [R0500054]
[b] [R0300234-1]; the rat ADME study and bile study
[c] Trace or not detected
[d] [R0500055]
[e] [R0500294]
[f] 0-48 h
[g] [CAMN107A2104]

2.6.6 TOXICOLOGY

2.6.6.1 Overall toxicology summary

General toxicology:
The toxicity of oral administration of AMN107 was investigated in rats (4 and 26 weeks), dogs (4 weeks) and monkeys (39 weeks) following single dose or repeat dose treatment (for the length of duration as indicated). Single dosing via IV bolus or infusion in rats was without remarkable findings. Daily treatment of AMN107 up to 600 mg/kg/d was tolerated. The common findings included: GI related clinical signs (fecal changes, emesis, salivation, oral discharge), decreased body weights/food consumption, decreased erythroid parameters (RBC, HGB, Hct) with or without increase in erythrocyte counts, increased white counts (total and differentiated), prolonged APTT in monkeys, increased ALT, ALP, total bilirubin (bilirubinuria in female dogs), cholesterol and triacylglycerides. The target organs were liver (Kupffer cell hypertrophy, vacuolation, fibrosis), bile duct (hyperplasia/proliferation) and/or gall bladder (increased luminal mucus), kidney (such as hyaline droplet in proximal tubules in male rats, tubular basophilia, vacuolation, mineralization, fibrosis), lung (interstitial inflammation macrophage accumulation), heart (cardiomyopathy, focal mesothelial cell proliferation), and spleen (hemorrhage, fibrosis, lymphoid hypocellularity). Uterine dilation was seen in rats after 26 week treatment, and findings in pancreas (acinar degeneration, inflammation) and thyroid (fibrosis, hyperplasia) appeared later in 39 week study in monkeys. There were no hemodynamic or EKG changes in the dog or the monkey.

Genetic toxicology:
AMN107 was not mutagenic in bacterial Ames test (*Salmonella typhimurium* TA98, TA97a, TA100, TA102 and TA1535), and was not clastogenic in the chromosome aberration teat in human peripheral blood lymphocytes. AMN107 did not induce DNA damage/increased migration in the Comet assay. All the results of the *in vitro* studies remained the same with the presence or absence of rat liver S9-mix. Orally administered AMN107 up to 2000 mg/kg did not induce bone marrow toxicity and did not induce micronuleus formation.

Carcinogenicity:
Not conducted.

Reproductive toxicology:
The reproductive and developmental toxicology (fertility and early embryonic development, and embryofetal development) of AMN107 was investigated in both rodent (rats) and non-rodent (rabbit). AMN107 treatment did not affect male or female fertility, mating index or pregnancy in rats. Similar results were observed in female rabbits. In rats, embryofetal toxicities were seen in the absence of maternal toxicity (decreased gestation weights and gravid uterine weights). AMN107 caused dose-dependent embryotoxicity (increased post-implantation loss and early (total) resorption in rats and rabbits, decreased fetal viability and little size in rats, and abortion in rabbits), as well as fetal toxicity (visceral and skeletal malformations and variations in rats, and skeletal variation in rabbits). The data indicated that AMN107 was not teratogenic under the conditions of the studies.

Special toxicology:
AMN107 demonstrated a phototoxic potential when tested *in vitro* 3T3 NRU assay, but was not photosensitizing in the *in vivo* murine UV-LLNA assay.

2.6.6.2 Single-dose toxicity
Two intravenous studies in rats were reviewed and the findings are briefly summarized below.

Study 0510033: Intravenous dose-range finding study in rats

Objective:
The tolerability of AMN107 and its vehicle was investigated in rats (2M, 2F) after a bolus IV injection or IV infusion
Methods and results:
✧ Parameters

Mortality and clinical signs	Following administration
Body weight	On the days of administration
Toxicokinetic	Blood samples were collected at 5 min, 0.5, 2, 7, and 24 hr after administration.

✧ The treatment, allocation of the rats and results were as follows:

Study day	Treatment	Dose (mg/kg)	Dosage volume (mL/kg)	Animal	Findings
1	Vehicle A	0	10	M (#101, #102), F (#103, #104)	Cyanosis (1/4) in vehicle group
5	AMN107	20	8.3	M (#101)	Not remarkable in AMN107 group
36	Vehicle B	0	5 (bolus)	M (#101), F (#103)	Not remarkable (5 mL/kg bolus)
		0	10 (bolus)	M (#102), F (#104)	Reduced activity, recumbency (recovered within 1 hr) (10 mL/kg bolus or infusion)
39		0	10 (infusion)	M (#102), F (#104)	
42	AMN107	9	10 (bolus)	M (#101, #102), F (#103, #104)	Not remarkable, except the vehicle effect (AMN107 treated group)

Vehicle A: ethanol, PEG 300, Tween 80 and glucose (4.17%, 12.5%, 2.5% and 2.5%, respectively)
Vehicle B: ethanol, PEG, Cremophor and glucose (1.5%, 4.5%, 5% and 3.7%, respectively)
AMN107 (batch# 0523011, salt:base ratio 1.103): in vehicle A (2.4 mg/mL, pH ~5), in vehicle B (0.9 mg/mL, pH 4.5).

Note: AMN107 in vehicle A was not stable and precipitated within 15 min after preparation. Only one rat received AMN107 in vehicle A and there were no findings in this rat. No weight or food intake changes were found in vehicle or AMN107 treated rats.

✧ The TK parameters of AMN107 at 9 mg/kg were tabulated in the table below:

	C_{max} (µg/mL)	AUC_{0-24h} (µg•h/mL)	C_{max}/dose	AUC_{0-24h} /dose	T_{max} (h)
Males (n=2)	37.7	76.8	1.89	3.84	0.083
Females (n=2)	27.8	110	1.39	5.49	0.083

Study 0510081: Single-dose intravenous toxicity study in rats

This was an OECD GLP-compliant study. Forty rats (━ :W1 (Han), n=5/sex/group/study) were treated with either vehicle (ethanol, PEG, Cremophor and glucose (1.5%, 4.5%, 20% and 74%, v/v, respectively)) or AMN107 (9 mg/kg) via a single IV bolus injection (10 mL/kg). The 20 rats in the interim study group was sacrificed 24 hr post dosing, while the remaining rats in the main study group were observed for 15 days post doing. The following investigations were performed: mortality, clinical signs, body weight, food consumption, hematology, clinical chemistry, organ weight, gross and histopathology, and toxicokinetics (see Study# 0510033). Other than the vehicle effect (recumbency) there were no findings in in-life observations. Findings in hematology and clinical chemistry were incidental. Several rats, vehicle or AMN107-treated animals, were found with ischemic-associated minimal acute or subacute focal necrosis in the brain upon histopathological examinations. Since only one dose of AMN107 was used, without the information of dose-relationship the significance of the findings is uncertain.

The TK parameters of AMN107 (n=2/sex/group/time point) were tabulated in the table below:

	C_{max} (µg/mL)	AUC_{0-24h} (µg•h/mL)	C_{max}/dose	AUC_{0-24h} /dose	T_{max} (h)
Males	31.5	68.7	3.5	7.63	0.083
Females	30.1	103	3.34	11.4	0.083

2.6.6.3 Repeat-dose toxicity

Study title: 4-Week oral (gavage) toxicity study in rats with a 4-week recovery period.

Key study findings:

- AMN107-related findings included decreased weight gain (19-24% lower than the control) in male rats at 60 mg/kg/day, and increased heart weight (12-15% absolute and 18-19% relative) in both male and female rats at 60 mg/kg.

Note: This study was reviewed in IND 69764 (Review #1). The IND review is reformatted and incorporated in this NDA review.

Study no.: 0370146
Volume#, and Page number: Volume #4 and page #8-715 to 8-960
(Note: in the NDA submission: Electronic module (pharmtox\tox\0370146.pdf))
Conducting laboratory and location: Novartis Pharmaceuticals Corporation, One Health Plaza East, Hanover, NJ 07936-1080.
Date of study initiation: November 11, 2003
GLP compliance: yes.
QA report: yes (x) no ( ).
Drug, lot #, and % purity: AMN107 hydrochloride, lot #0351002, purity: [redacted]

Methods:

Species: IGS Wistar Hannover rats; [redacted]: WI (Glx/BRL/Han) IGS BR
n: 10/sex/group, plus 6 to the control and 60 mg/kg group as recovery animals.
Age/Weight: 8 weeks/163-279 gm
Doses: 0 (control), 6, 20, 60 mg/kg (groups 1, 2, 3 and 4, respectively).
Schedule: Once daily x 28 d. The recovery animals (groups 1 and 4): dosed x 28 d + observation x 28 d (no treatment).
Route: Oral by gavage (5 mL/kg).
Formulation/vehicle: A solution in vehicle: 0.5% w/v hydroxypropyl methylcellulose (HPMC). The concentration was calculated to give a constant dose volume of 5 mL per kg body weight for each dose level (see table below).

Table 3-1 Study design, animal allocation and test article doses

Group	Number/sex	Animal numbers males	Animal numbers females	Dose (mg/kg/day) Base/Salt*	Concentration (mg/mL) Salt*
1	10	1001-10	1501-10	0	0
Control	+6 recovery	1011-16	1511-16		
2	10	2001-10	2501-10	6/6.4	1.3
Low					
3	10	3001-10	3501-10	20/21	4.2
Mid					
4	10	4001-10	4501-10	60/64	12.8
High	+6 recovery	4011-16	4511-16		

*Salt/base ratio is 1.069.

Dose justification:
Dose levels used in the following study were selected based upon previously conducted 2-week oral (gavage) dose range-finding toxicity study [redacted] For rats treated with 30, 100 and 300 mg/kg/day, weight loss and reduced food consumption were seen at all doses. Findings in hematology, clinical chemistry, and histopathology mostly occurred at doses ≥ 100 mg/kg/day. Erythrophagocytosis within the medullary sinuses of lymph nodes and ovarian follicular or luteal cysts were noted at doses ≥ 30 mg/kg/day.

Observations and times:

Clinical signs: Twice daily for mortality, moribundity and gross abnormality. Detailed physical examination: twice daily on each day of dosing days and at least once on non-dosing days.
Body weights: Once prior to treatment and weekly thereafter.
Food consumption: Weekly pre-study and throughout the remainder of the study.
Ophthalmoscopy: On all animals during pretest and on all control and Group 4 animals during Week 4 with an indirect ophthalmoscope.
Electrocardiography: Not performed.
Hematology: In Week 4 and on Day 57.
Clinical chemistry: In Week 4 and Day 57.
Urinalysis: Up to 5 hour urine samples were collected in Week 4 and Day 57.
Gross pathology (necropsy): Scheduled sacrifice: Day 29 or after recovery period (D57).
Organ weights: At scheduled sacrifice. See Histopathology inventory
Histopathology: Day 29 or Day 57. All tissues collected from all non-recovery animals in Groups 1 and 4 were subjected to histopathological examination. In addition, the following tissues from Groups 2 and 3 and recovery animals were also examined: cervix, heart, kidneys, lymph node-bronchial, mandibular, mesenterc, ovaries, thyroid glands, uterus and vagina (inventory: see results).
Toxicokinetics: Blood samples (1 mL) were collected from non-recovery animals on Day 1/2 and Day 28/29, at 0.5, 1, 3, 7, and 24 hours post-dose (n=2/ time point). LLOQ was 4.98 ng/mL.

Results:

Mortality /Moribundity	No mortality or moribundity.
Clinical signs	Unremarkable, except salivation in three Group 4 females (#4501, 4503, 4514).
Body weights	Reduction in group mean body weight (6% reduction from the control, data not shown) was seen in Group 4 males at the end of treatment. The mean weight gain was reduced significantly in treated Group 4 males. The comparison among dose levels was summarized in the table below. The finding resolved at the end of recovery period.
Food consumption	Unremarkable

- Reduction (%) of group mean body weight gain in AMN107-treated males as compared to the control:

Dates/Dose	Group 2	Group 3	Group 4
D8	12 (NS)	15 (NS)	23
D15	16	13 (NS)	24
D22	13 (NS)	9 (NS)	19
D29	11 (NS)	11 (NS)	22
D41*			10 (NS)
D55*			9 (NS)

Note: the numbers reflect % reduction compared to the control. *recovery period, NS: non-significant.

Ophthalmoscopy: not remarkable

Electrocardiography: not performed

Hematology:

	Males			Females		
	Week 4			Week 4		
	Group 2	Group 3	Group 4	Group 2	Group 3	Group 4
WBC ↑					29	31
Lymph ↑						28
Mono* ↑			53			55
LUC ↑					60	80
Retic % ↑			13			
Retic absolute ↑			12			

LUC: large unstained cells. *: Still ↑ 27% in male Group 4 recovery animals.

Clinical chemistry: Unremarkable

Urinalysis: Unremarkable

Organ weights:

Drug-related absolute and relative organ weight changes expressed as % change of control:

	Males							Females						
	Day 29						Day 57 (recovery)	Day 29						Day 57 (recovery)
Group	Group 2		Group 3		Group 4			Group 2		Group 3		Group 4		
	gm	% BW	gm	% BW	gm	% BW		gm	% BW	gm	% BW	gm	% BW	
Adrenal ↑												13	13	
Heart ↑					12	19						15	18	
Kidney ↑					8	15							8	
Liver ↑										11	15	13	16	
Prostate ↓			9	7	20	14	% BW ↑ 17%							
Spleen ↑			13	16	5	11	% BW ↑ 14%							
Thymus ↑							% BW ↑ 25%	12	14	9	13	↓ 8	↓ 6	
Thyroid ↑	12	18	23	28	4	10	% BW ↑ 29%	9	11	4	11	↓ 30	↓ 25	% BW ↑ 14%

Comment:

- The increased organ weight in heart, kidney, liver (females), thymus and thyroid, or decreased thymus and thyroid weight in females mostly resolved in the recovery period. There was no strong support from histopathological findings for weight changes in these organs.

Gross pathology

The findings included: skin (alopecia, hair loss), eye (opacity, dark or discoloration), and lymph nodes (branchial, pancreatic, mediastinal, mesenteric, mandibular: discoloration).

	Males				Females			
	Group 1	Group 2	Group 3	Group 4	Group 1	Group 2	Group 3	Group 4
Liver: dark focus	1							
Pale focus						1		
Thymus: multiple red foci	1							
discoloration						1		
Skin: alopecia		1						
hair loss						1		1
Epididymides; head nodule				1				
Eye: opacity		1					1	1
dark, discoloration, enlarge				3				
Kidney: dilatation		1						
tan focus				1				
Lymph node: Bronchial			1					
enlarge								
Lymph node: Pancreatic				1				
discoloration, dark								
Lymph node: Mediastinal				1				
discoloration								
Lymph node: Mesenteric				3				1
discoloration								
Lymph node: Mandibular				2				
discoloration								
Uterus: dilatation								1

Most findings were with group 4, especially discoloration in the lymph nodes. The macroscopic findings resolved in the recovery animals, except that discoloration in lymph nodes was found in 2/10 male group 4 animals.

Histopathological findings:

Histopathology / Group	Group 2		Group 3		Group 4		Recovery (G4)	
Sex	M	F	M	F	M	F	M	F
Number of animals	10	10	10	10	10	10	6	6
Eyes							[1]	[1]
minimal to moderate anterior chamber exudate	1		1	1			1	
minimal to marked keratitis	1		1	1			1	
minimal to moderate unilateral keratitis					2	1		
minimal to slight retrobulbar inflammation	1				2			
minimal to moderate unilateral retrobulbar hemorrhage					1		1	
slight unilateral anterior chamber exudate					2			
Harderian gland	[1]	[1]	[1]	[0]	[10]	[10]		
slight chronic focal inflammation					1			
minimal to moderate inflammation	1		1		1		1	
slight hemorrhage					1			
Lacrimal gland	[0]	[0]	[0]	[0]	[10]	[10]		
minimal leukocytic infiltrate					1			
minimal acinar degeneration					1			
Lung	[0]	[0]	[0]	[0]	[10]	[10]		
minimal chronic focal pleura inflammation					1			
minimal focal type II cellular hyperplasia						1		
minimal focal hemorrhage					1			
minimal hemorrhage*					1			
Duodenum	[0]	[0]	[0]	[0]	[10]	[10]		
minimal goblet cells decrease						1		
minimal leukocytic infiltrate						1		
Ileum	[0]	[0]	[0]	[0]	[10]	[10]		
minimal Peyer's patch hyperplasia					1			
Cecum	[0]	[0]	[0]	[0]	[10]	[10]		
minimal leukocytic infiltrate					1			
Esophagus	[0]	[0]	[0]	[0]	[10]	[10]		
minimal muscularis regeneration					1	1		
minimal leukocytic infiltrate					1			
minimal muscularis degeneration						1		
Heart								
minimal cardiomyopathy	1		3		4	3		
minimal mononuclear infiltrate	1							2
Kidney								
minimal focal fibrosis		1				1		
minimal to moderate hyaline droplets*	6		8		8		4	
minimal cyst	1							
minimal tubular pigment				1				
moderatefocal cyst					1			
minimal basophilic tubules*	3		1	1	4	2		
Lymph node: Bronchial							[5]	[5]
minimal lymphangiectasis			1		1			
minimal leukocytic infiltrate					1			

Lymph node: Mandibular								
minimal to moderate erythrocyte accumulation*	2		4	1	6	4	3	1
minimal macrophage pigment				1				
minimal plasma hyperplasia				1				
minimal lymphoid hyperplasia						1		
minimal sinusoidal histocytosis			1					
Lymph node: Mesentaric								
minimal to slight erythrocyte accumulation			1		3	2		
minimal macrophage pigment							1	
minimal lymphangiectasis			1			1		
Lymph node: pancreatic								
minimal macrophage pigment					1			
slight erythrocyte accumulation					1			
Nerve: optic	[0]	[1]	[0]	[0]	[0]	[1]		
moderate macrophage infiltrate		1						
minimal unilateral degeneration						1		
Pancreas	[0]	[0]	[0]	[0]	[10]	[10]		
minimal periductoral inflammation						1		
minimal duct epithelial hyperplasia						1		
minimal duct focal fibrosis					1	1		
minimal cyst						1		
Spleen	[0]	[0]	[0]	[0]	[10]	[10]		
minimal lymphoid hyperplasia						1		
slight congestion						1		
Stomach	[0]	[0]	[0]	[0]	[10]	[10]		
minimal glandular regeneration					1			
minimal leukocytic infiltrate					1			
minimal nonglandular hyperkeratosis						1		
minimal erosion					1	1		
minimal nonglandular edema						1		
minimal glandular debris					1			
Thyroid								
minimal mononuclear infiltrate				1				
minimal ultimobranchial cyst						3		
minimal cyst					2	2		
Thymus	[0]	[0]	[0]	[0]	[10]	[10]		
minimal increased apoptosis						1		
minimal macrophage accumulation					1			
Epididymides	[0]		[0]		[10]			
slight sperm granuloma					1			
Ovary		[10]		[10]		[10]		[6]
minimal luteal cyst				1				
minimal corpus luteam hemorrhage		1				1		
minimal follicular atresia								1
minimal cyst						1		
Uterus		[10]		[10]		[10]		[6]
minimal luminal dilatation						1		
Vagina		[10]		[10]		[9]		[6]
slight apoptosis								1
minimal to slight vacuolation		1		2				

Note: The number in the parenthesis indicates the number of animal examined for a particular tissue/organ. *: findings also in the control animals, see below for details.

- Comments:
  - The finding of hyaline droplets in the proximal tubules was specific to male rats, as an indication of the initial phase of the inducible male rat $\alpha_{2\mu}$ globulin nephropathy syndrome. This finding partially resolved.
  - Target organs also included lymph nodes, eyes (lacrimal and Harderian glands), thyroid and heart.

Toxicokinetics:

Males:

	Day 1			Day 28		
Group	Group 2	Group 3	Group 4	Group 2	Group 3	Group 4
Dose (mg/kg/d)	6	20	60	6	20	60
C_{max} (ng/mL)	1092	3660	3870	1158	4000	9240
C_{max}/dose	182	183	64.5	193	121	154
$AUC_{0\text{-}24h}$ (ng•h/mL)	6240	44400	52080	6900	21000	120000
$AUC_{0\text{-}24h}$/dose	1040	2220	868	1150	1050	2000

Females:

	Day 1			Day 28		
Group	Group 2	Group 3	Group 4	Group 2	Group 3	Group 4
Dose (mg/kg/d)	6	20	60	6	20	60
C_{max} (ng/mL)	1512	2420	4020	1368	3200	13200
C_{max}/dose	252	200	67.0	228	160	220
$AUC_{0\text{-}24h}$ (ng•h/mL)	12720	34860	60000	11220	46200	187200
$AUC_{0\text{-}24h}$/dose	2120	1740	1000	1870	2310	3120

  - On Day 1 both male and female rats at 60 mg/kg showed approximately one-half AUC/dose and C_{max}/dose compared to the two lower doses. However, on Day 28, while the C_{max} maintained unity among doses in both sexes, AUC/dose was elevated at 60 mg/kg.
  - Female rats showed more exposure (AUC/dose) to the repeated oral administration of AMN107 than male rats.

Summary of the individual study:

- Overall, the oral treatment of AMN107 in the dose range of 6-60 mg/kg/day was tolerable. Most of toxicity, such as weight loss, reduced food consumption and histopathological findings resolved at the end of recovery period.
- There were unremarkable changes in hematology, clinical chemistry and urinalysis parameters.
- The targeted organs of AMN107 toxicity included: kidney (hyaline droplets), lymph nodes (branchial, pancreatic, mesenteric and mandibular lymph nodes discoloration), heart, eye, and lacrimal/Harderian gland. Most changes were minimal and resolved during recovery period.

Study title:
AMN107: a 26-week oral (gavage) toxicity study in rats with a 4-week recovery period

Key study findings:
- The AMN107 related toxicity, mainly at 60 mg/kg, included: decreased body weights/food intake, hematological effects (↓erythroid parameters and ↑ total and differentiated white blood cell counts), and increased total cholesterol (males and females) and triglycerides (females), as well as increased hear weight (11% absolute weight in males at 60 mg/kg, and 12-19% reltive weight in both malae and female rats at ≥ 20 mg/kg).
- The main target organ was uterus.

Study no.: #0580158 ([redacted] .053.12)
Volume #, and page #: Electronic module (pharmtox\tox\0580158.pdf)
Conducting laboratory and location: [redacted]

Date of study initiation: April 20, 2005
GLP compliance: Yes
QA report: yes (X) no ( )
Drug, lot #, and % purity: AMN107, Lot # 0523025, purity: [redacted]

Methods
Doses: 0 (control), 6, 20 and 60 mg/kg (free base, as Groups 1, 2, 3 and 4)
Species/strain: IGS Wistar Hannover rats; [redacted] WI(Han)IGS BR
Number/sex/group or time point:
Main study: n=20/sex/group; Ten per sex per group of these animals were also used for toxicokinetics
Recovery animals: n=10/sex in Groups 1 and 4
Satellite groups used for genomic assay study: 6/sex/group (Groups 1 and 4 only)

Route, formulation, volume: oral gavage at dose volume of 5 mL/kg
- Formulation: AMN107 suspensions at dose concentrations of 1.2, 4 and 12 mg/mL for Groups 2, 3, and 4, respectively. (Note: Doses were corrected for percent active AMN107 moiety (96.4%). Salt/base ratio for AMN107 was 1.103.)
- Vehicle: 0.5% (w/v) hydroxylpropyl-methylcellulose (0.5% HPMC) in water for injection, USP.

Age: ~7-9 weeks
Weight: 164-250 g
Schedule: Once daily for 26 consecutive weeks. The main study was followed by a 4-week recovery period.

Dose justification: Dose selection is based on a previous study (Study # 0370146, see above), in which oral administration of a dose of 60 mg/kg (daily, for 4 weeks) resulted in a significant decrease in body weight (- 6%) and weight gain (- 19% to -24%) in males. Other treatment related findings included changes in organ weights (↑ heart, kidney, liver and ↓